Survey on Wheel Slip Control Design Strategies, Evaluation and Application to Antilock Braking Systems

Pretagostini, Francesco; Ferranti, Laura; Berardo, Giovanni; Ivanov, Valentin; Shyrokau, Barys

DOI
10.1109/ACCESS.2020.2965644

Publication date
2020

Document Version
Final published version

Published in
IEEE Access

Citation (APA)
Pretagostini, F., Ferranti, L., Berardo, G., Ivanov, V., & Shyrokau, B. (2020). Survey on Wheel Slip Control Design Strategies, Evaluation and Application to Antilock Braking Systems. IEEE Access, 8, 10951-10970. https://doi.org/10.1109/ACCESS.2020.2965644

IEEE Access
Multidisciplinary | Rapid Review | Open Access Journal

Received December 30, 2019, accepted January 7, 2020, date of publication January 10, 2020, date of current version January 17, 2020.

Digital Object Identifier 10.1109/ACCESS.2020.2965644

Survey on Wheel Slip Control Design Strategies, Evaluation and Application to Antilock Braking Systems

FRANCESCO PRETAGOSTINI[1], LAURA FERRANTI[1], GIOVANNI BERARDO[2], VALENTIN IVANOV[3], AND BARYS SHYROKAU[1]

[1]Department of Cognitive Robotics, Delft University of Technology, 2628 CD Delft, The Netherlands
[2]Chassis Control Department, Toyota Motor Europe, B-1930, Zaventem, Belgium
[3]Automotive Engineering Group, Technische Universität Ilmenau, 98693 Ilmenau, Germany

Corresponding author: Barys Shyrokau (b.shyrokau@tudelft.nl)

This work was supported in part by the Development from the European Union's Horizon 2020 Research and Innovation Programme under the Marie Skłodowska-Curie under Agreement 734832, and in part by the the Dutch Science Foundation NWO-TTW Foundation within the SafeVRU Project under Grant 14667.

ABSTRACT Since their introduction, anti-lock braking systems (ABS) have mostly relied on heuristic, rule-based control strategies. ABS performance, however, can be significantly improved thanks to many recent technological developments. This work presents an extensive review of the state of the art to verify such a statement and quantify the benefits of a new generation of wheel slip control (WSC) systems. Motivated by the state of the art, as a case study, a nonlinear model predictive control (NMPC) design based on a new load-sensing technology was developed. The proposed ABS was tested on Toyota's high-end vehicle simulator and was benchmarked against currently applied industrial controller. Additionally, a comprehensive set of manoeuvres were deployed to assess the performance and robustness of the proposed NMPC design. The analysis showed substantial reduction of the braking distance and better steerability with the proposed approach. Furthermore, the proposed design showed comparable robustness against external factors to the industrial benchmark.

INDEX TERMS Road vehicles, vehicle safety, antilock braking system, wheel slip control, model predictive control.

I. INTRODUCTION

Anti-Lock Braking System (ABS) is among the most challenging topics of wheel slip control (WSC) design. ABS is an active safety technology used to control wheel dynamics during severe braking. The system aims at maximizing braking performance while keeping the vehicle's ability to steer. The ABS control objective is achieved by the modulation of the applied brake pressure.

Being a safety system, ABS must satisfy a wide range of requirements, [1] It must:

- Maintain steering response and vehicle stability at all times, regardless of road conditions;
- Utilize the friction between tires and road surface towards maximizing the braking performance;
- Be fully functional throughout the vehicles speed range;
- Allow for rapid adaptation to changes in road friction.

ABS design is complicated by uncertainties, measurement noise, parameter variations, and nonlinearities [2], [3]. For example, relevant fundamental quantities (such as vehicle velocity, longitudinal wheel slip, and tire-road friction coefficient) are highly noisy and need to be estimated. Depending on road conditions, the maximum allowable braking force may vary over a wide range of values. On rough roads, the wheel slip ratio can be changed rapidly due to tire bouncing. Furthermore, due to variations in the disc-pad friction coefficient, the brake torque-pressure relation is nonlinear. In addition to this, the plant to be controlled (i.e., an elastically suspended wheel, a braking servo system, and actuators) introduce significant delays that limit the controller's bandwidth. Lastly, the main difficulty arising in the design of

The associate editor coordinating the review of this manuscript and approving it for publication was Jianyong Yao.

an ABS control law, is the strong nonlinearity of the tire (tire force saturation).

Since the first reliable ABS applications in late 1970s, a wide variety of approaches have been proposed for vehicles to overcome the challenges above. This paper contributes to the current literature by introducing a critical overview and analysis of the state of the art in ABS control design (Section II). An additional contribution, is the list of key performance indicators (KPIs) and scenarios by which to benchmark and validate any proposed ABS design (Section III), with the aim of providing guidelines for future research in this area. Motivated by the conclusions of the review of the state of the art, a Nonlinear Model Predictive ABS Controller is presented and validated through the designed KPIs and compared with respect to a more classical approach (Sections IV). The novelty of the proposed controller is the usage of reconstructed wheel force information in the prediction horizon allowing to achieve a better tracking performance compared to the industry-used logic and the reduction of computational load.

II. SURVEY OF CONTROL STRATEGIES FOR WHEEL SLIP CONTROL

The design of wheel slip control systems is highly dependent on the brake actuators characteristics. Firstly, the brake actuator characteristics is discussed after this, focus is given to the different control approaches found in literature.

The most common brake system layout of passenger cars is Hydraulically Applied Brakes (HAB), shown in Fig. 1a. Brake servo assistance is generated by the brake booster. The brake booster is a hollow housing with a movable rubber diaphragm creating two chambers, one of which is pressure varying. The process of filling up the rear chamber with atmospheric air when the brakes are applied introduces significant delays in the brake actuation. The ABS function is realized by controlling the on/off solenoid valves. The system uses the volume accumulator to dump pressure and the driver force to increase it, while the pump is only used to bring the excess fluid back into the master cylinder reservoir (Fig. 1a). In this layout, pressure modulation is usually realized in a stairway-fashion making it most suitable for threshold-based, fuzzy logic and neural-network control.

Demand on brake blending in electric vehicles is causing the gradual shift from conventional hydraulic to Electro-Hydraulic Brake (EHB) systems. These systems are generally characterized by a faster response compared to conventional hydraulic systems and allow for continuous pressure modulation. HAB response time can be found in the range of 200 to 400 ms [4] depending on the on the size of the brake system and the manufacturer, while EHB response is between 60 to 100 ms [5]. The system's key element of EHB systems is the boost valve, an electronically controlled proportional valve, downstream the high-pressure accumulator, as shown in Fig. 1b. By proportionally opening and closing this element, it is possible to achieve a specific target pressure. To control solenoid coil, direct current control

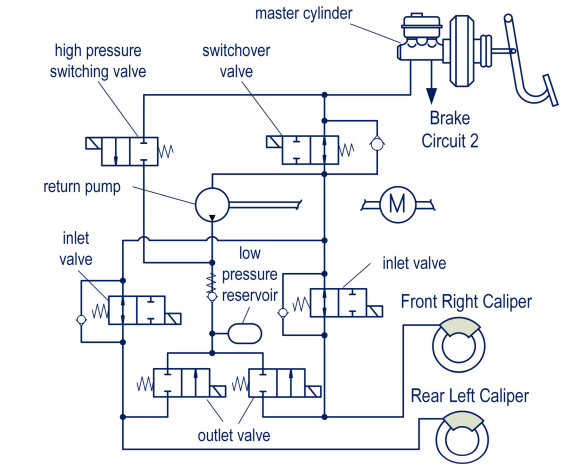

(a) Conventional hydraulic ABS hardware, half view (adapted from [1]).

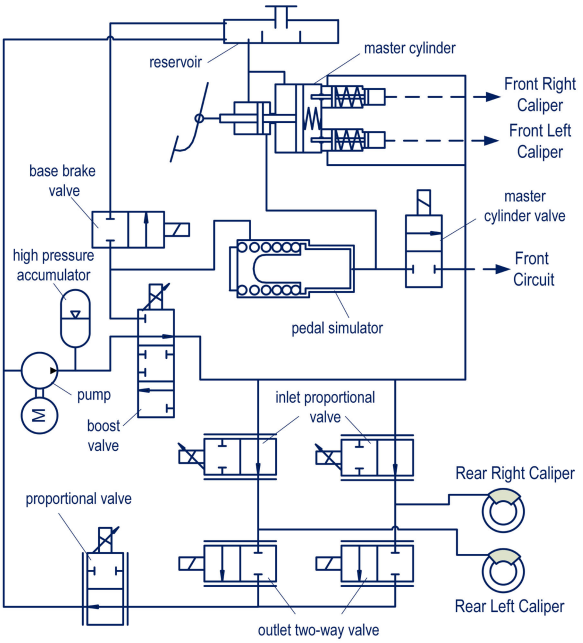

(b) Electro-hydraulic ABS hardware, half view (adapted from [21])

FIGURE 1. Brake system layouts.

or pulse width modulation (PWM) method are commonly used [6]. More advanced control methods of hydraulic system can be found in [7], [8].

For hybrid and electric vehicles, an electric motor can be used to generate additional brake torque demand allowing the regenerative braking [9]. Depending on the powertrain layout, blending between frictional brake system and electric motor(s) can be designed in the several ways. Commonly for central axle location of the electric motor, high-frequency brake demand is generated by frictional brake system, e.g. for hybrid [10] or electric [11] vehicle. The application of the single axle electric motor to generate high-frequency demand has been investigated, e.g. for a hybrid sport utility vehicle (SUV) [12], an electric commercial vehicle with a pneumatic brake system [13], passenger electric vehicle [14]. The main

limitation to use the single axle electric motor for wheel slip control is related to dynamics of the transmission, the final axle and the differential.

In the case of on-board or in-wheel electric motors, the dynamics of mechanical components (e.g. half-shaft dynamics for on-board electric motor) have a lesser effect on the performance of wheel torque modulation. From the perspective of wheel slip control, due to a faster response of the electric motor compared to the frictional brake system, high-frequency brake demand can be more effectively realized by the electric motor and so, a continuous wheel slip control can be achieved [15], [16].

The literature, related to the ABS control, traditionally addresses one of the following quantities used as the wheel dynamics parameters: (i) wheel acceleration $\dot{\omega}$ and (ii) longitudinal wheel slip λ.

On one hand, the *wheel-acceleration control* has the benefit that the wheel acceleration, as control parameter, can be estimated more simply than wheel slip, this can be done by using wheel-encoder measurements. Furthermore, wheel-acceleration control allows wheel slip to keep close to the optimal point, without explicitly using the value of this point.

On the other hand, assuming robust estimation of longitudinal wheel slip, the *wheel slip control* is simpler from a dynamical point of view and has the feature that the applied torque converges to a fixed value. Hence, the controlled system shows lesser oscillations compared to wheel-acceleration control designs [17], [18]. The controller, however, is highly sensitive to set-point selection. Hence, the controller requires a set-point adaptation strategy based on the road conditions [19]. In addition to this, the longitudinal wheel slip requires information about the vehicle velocity. Given that direct measurement of this quantity is quite expensive to be used for mass-production cars, the velocity is obtained via estimation, making longitudinal wheel slip control highly sensitive to measurement noise [20].

Independently from the selected variant of control strategy, the WSC should provide reliable generation of the *reference wheel slip ratio and its adaptation to driving conditions*. But only few published studies are known in this area, in particular, the authors in [22] proposed reference slip estimation using the bootstrap Rao-Blackwellized particle filter based on the signals from the wheel speed sensors, accelerometer and GPS. Estimation of the reference slip is also discussed and validated in simulation in [23], where wheel slip dynamics is handled as the second-order system based on LuGre friction model. Feedback linearizing control is used in [24], where the optimal wheel slip area is determined by the extremum seeking algorithm based on the online optimization method, where an uncertain plant with unknown parameters is considered. However, as it can be concluded from the analysis of published research studies, robust and real-time capable methods of the reference wheel slip estimation are mainly based on the polynomial fitting algorithms. As it was demonstrated in [25], [26], this method allows determination of extremum position using conventional on-board vehicle sensors and applying methods requiring reasonable computational resources. However, there is limited information in relevant publications about the integration of the slip target adaptation mechanisms [27] into the overall control architecture.

To estimate the *vehicle velocity* or *ABS reference velocity* [28], the problem has traditionally been tackled by pursuing one of the following approaches: (i) devising algorithms based on intuitive procedures linked to the physics of problem (e.g., underbraking the rear wheels to use them as a sensor to control the front wheels), (ii) setting up black-box approaches based on input/output data (e.g., fuzzy logic or neural networks), and (iii) stating model-based filtering problems solved via classical identification techniques and observer design methods (e.g. Kalman filters) [29]. The continuous control system can be potentially realized with many approaches, starting from well-known PID algorithms up to complex hybrid control methods.

Remark 1: In the last decade, much effort has been spent to develop sensors or estimators to provide tire force information to improve ABS control design. Wheel force information would allow for easy estimation of the peak friction coefficient. Additionally, the availability of the tire forces would benefit model-based optimal control designs, such as model predictive control (MPC), from the computational point of view. This information allows the controller to eliminate the tire model and, consequently, some nonlinearities and tedious trigonometric functions. In this respect, *load-sensing technology* allow for the reconstruction of tire forces, with sufficient accuracy and bandwidth, and so recent research is hoped to lead to commercialization in the coming decade [30], [31]. The proof-of- concept of load-sensing technology to ABS application was demonstrated for intelligent tires [32] via simulations and for load-sensing bearings in laboratory conditions using a tire test rig [33] and field testing [34].

Considering typical WSC systems requirements in terms of real-time applicability and robustness to manoeuvre-/road-related uncertainties, it is difficult to select a priori a more suitable control technique [35], [36]. The remainder of the section reviews the *main* ABS control trends proposed by researchers and OEMs. Two macro directions are identified. The first direction (dynamic threshold-based, fuzzy-logic and neural-network controllers) achieves the control objective by discretely modulating brake pressure for each wheel. The second direction (PID, linear quadratic, sliding mode, robust and predictive controllers) assumes the possibility of continuously modulating brake pressure and, thus, brake torque. The existing control approaches are compared with the focus on their applicability to ABS applications.

A. THRESHOLD-BASED (RULE-BASED) CONTROLLERS

Logic threshold-based controllers are widely used in ABS applications. The advantages of these control methods come from the heuristic, tuneable control laws, and low hardware requirements (such as the HAB in Fig. 1a). Rules are

identified from practical experience as well as intensive simulation studies. The approach has good performance in practice but requires extensive testing for fine tuning the control logic, starting from initial look-up tables values. Additionally, since threshold-based control uses a heuristic approach, the stability assessment by means of common stability analysis theory is debatable. Furthermore, the robustness assessment needs to be done via experiments on the target vehicle.

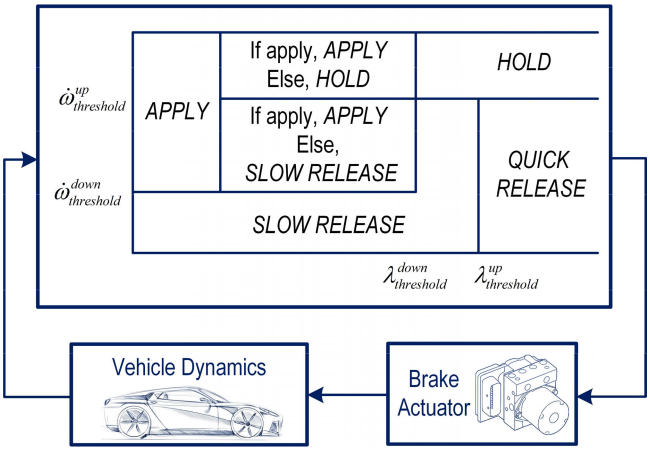

FIGURE 2. Logic threshold controller (adapted from [39]).

Threshold-based algorithms (Fig. 2) can be represented using the concept of Finite State Machines (FSM). Most states (each state is associated with a certain control action) are defined a-priori and the jumps from one state to the other are triggered when the control variable exceeds a predefined threshold. Three control actions of brake pressure are generally defined: (i) apply, (ii) release, and (iii) hold. A more detailed explanation of the working principles behind these algorithms can be found in [29], [37], [38].

Majority of industrial ABS systems fit in this category. Dynamical values of slip and deceleration, or a switching surface defined using a weighted sum of the two are commonly used [40]. In addition, given that the road conditions vary over a large range of friction levels, the thresholds need to be redefined for each of them (i.e., dry, wet, snow, etc.). As a result, the logic is adapted based on the output of a friction estimator. Furthermore, the inclusion of rules related to the functions of jerk compensation, yaw moment build-up delay for μ-split, braking-in-the-turn, braking on banked roads, rough road and road disturbance detection, and many others [1] increases complexity to the finite state machine. Consequently, the number of tuning parameters for a real application is incredibly high. This conclusion is supported by [19], [41]. The authors present a five-phase hybrid controller [19] using wheel deceleration logic-based switching and evaluate the design by means of Poincare' maps and limit cycle analysis. The acceleration-based switching thresholds are defined based on the analysis of the phase plane evolution of the system. The assumption is that the μ-curve maximum (possibly unknown) remains unchanged during the whole braking. A later study investigated the possibility of a μ-transition in friction during the manoeuvre and propose an eleven-phase strategy [41]. This approach implies a much higher number of tuneable parameters and could not be developed with the same mathematical soundness that facilitated the tuning in the simpler approach.

The authors of [17] revise the controller presented in [19] (to account for previously neglected effects) and test it on a tire-in-the-loop experimental setup. The aim was to make the algorithm robust to measurement noise without neither excessively increasing the triggering thresholds (which causes the controller to be non-reactive) nor by just heavily filtering the acceleration (which introduces delays). They use pressure-derivative profiles to anticipate the delays introduced by the processes mentioned above. This, however, introduces additional tuning parameters and the reduction of the pressure derivative, when approaching the switching threshold, due to time delays, is not able to prevent acceleration from exceeding predefined thresholds.

B. FUZZY LOGIC CONTROLLERS (FLC)

The strong non-linearity of the tire behaviour, together with the often noisy and uncertain state variables motivate the research on fuzzy logic for ABS control problems.

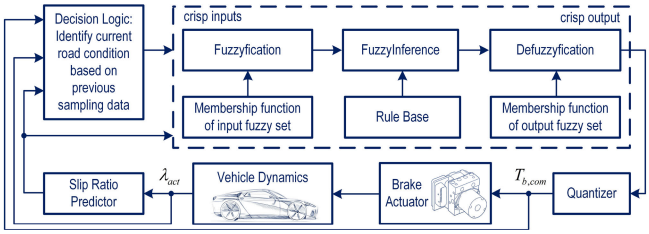

FIGURE 3. Fuzzy ABS controller (adapted from [2]).

Fig. 3 presents the structure of an ABS fuzzy controller. As the figure shows, error signals (*crisp inputs*) are created and compared with predefined fuzzy sets during the *fuzzification* process. A set of predefined logic rules create the input-output map. Finally, the output is *defuzzified*, that is, the defuzzified set is translated to an exact real value (*crisp output*).

Fuzzy logic can be easily blended with conventional control techniques, and the fuzzy control law can be calculated offline; however, the controller requires high memory storage. The available literature in this field ranges from fully fuzzy controllers to more traditional control strategies augmented by fuzzy systems. In [42], Layne et al. augmented a threshold-based controller with a fuzzy-model reference-learning control to maintain the desired fixed wheel slip in the presence of disturbances caused by adverse road conditions. This study showed that the fuzzy logic evaluation process ensures a rapid computation of the controller command, requiring less time and fewer computation steps than controllers with adaptive identification. The ABS system performance has also been investigated on a quarter vehicle

model with nonlinear elastic suspension, and the robustness of the overall controlled system has been evaluated for rough road conditions and in the presence of large measurement noise.

The work [2] by G. F. Mauer is among the most cited and discussed paper on fuzzy logic applied to ABS. This work presents a digital controller combining a fuzzy logic element and a decision logic network to identify the current road condition and generate a brake pressure signal based on current and past data of the wheel slip ratio and brake pressure. The author examined the ABS system performance on a quarter vehicle model with nonlinear elastic suspension and investigated the robustness on rough roads, while also including the effects of measurement noise. Then, the author benchmarked the performance of the FLC with a discrete PI controller. The main drawback of the proposed approach is that, compared to a PI controller, it requires a remarkably large number of parameters to be finely tuned to achieve the presented performance.

The authors in [43] presented an ABS FLC that includes the estimation of the tire-road friction coefficient and vehicle velocity using a recursive least square (RLS) method. The proposed method determines the optimal wheel slip using fuzzy logic considering wheel slip and friction coefficient. The authors tested the controller on a steal-belt-tire test bench with the brake system including a hydraulic pump, which was regulated by a proportional valve and fed a conventional brake piston connected with a brake calliper. No other control strategy was used to provide a clear performance assessment and, although the logic convincingly prevents wheel lock, evident oscillations are present on both the fuzzy controller's outputs.

Similar to the previous work, other FLCs have frequently been proposed to tackle the problem of ABS for the unknown environmental parameters [44], [45]. The large number of the fuzzy rules, however, makes the analysis comparable to the threshold controllers' case in terms of complexity. To mitigate this problem, some studies have proposed fuzzy-control design methods based on the sliding-mode control scheme (FSMC) [46], [47]. Since SMC brings a reduction of the system's order, FSMC requires relatively fewer fuzzy rules compared to FLC. Moreover, the FSMC system is more robust against parameter variation [47].

Although FSMC is an effective way to reduce the number of fuzzy rules, these would still be, as previously, tuned by the same time-consuming trial-and-error procedures. To tackle this problem, the authors in [48] combine a self-learning fuzzy sliding-mode control (with a fuzzy system mimicking an ideal control strategy) with a robust controller that compensates for the approximation errors (between the ideal and fuzzy controllers). The authors use Lyapunov-based tuning to guarantee stability and tested the controller on two simulation scenarios comparing its performance with SMC and FSMC designs. These simulations demonstrate that the self-learning approach requires less tuning providing similar results compared to FSMC and FLC. They are, however, based on oversimplifications, and it is hard to assess the controller behaviour in a real-life scenarious.

Lee and Zak introduced a genetic fuzzy ABS, which includes a non-derivative neural optimizer and fuzzy-logic components [49]. Specifically, they rely on the non-derivative optimizer from [50] to identify the road surface and to search for the optimal wheel slip. Based on these estimates, the FLC computes the brake torques. The authors also automated the tuning of the many fuzzy membership functions using a genetic algorithm. To check the outcome of tuning process, they tested the FLC by applying randomly varying reference wheel slips. However, the final controller assessment is done using a simple linear vehicle simulator (neglecting tire and actuators dynamics) and only compared to the uncontrolled case.

Remark 2: In literature, extraneous to ABS, controllers with shape-changing membership functions have been proposed [51], [52]. This approach allows to substantially decrease the number of rules. However, a large pre-defined knowledge base is still required.

C. NEURAL NETWORKS CONTROLLERS (NNC)

Similar to FLCs, Neural Networks (NNs) create suitable control alternative to deal with nonlinearities and variability. Different from FLCs, NN controllers use test data (rather than tuning the rules and membership functions) to train the NN and approximate the system with its nonlinearities. A hidden layer of neural network is tuned (for example, by using gradient descent techniques) to match all the corresponding input-output pairs in the training set. The network complexity can be increased by adding more layers (deep NNs), according to the requirements of the application.

Tuning from training data is a general advantage of neural networks. For WSC tasks, however, this NN feature might result in a fundamental weakness. Neural-network-based methods have the premise that the physical system can be sufficiently instrumented during network training so that the effect of control actions can be accurately evaluated. In the context of ABS application, it would be tremendously costly to obtain the necessary data required to exploit the full capabilities of neural methods.

Davis et al. in [53] present an initial simulation-based study to determine the performance potential of a NN-type ABS controller. The aim was to determine whether the cost of carrying out neural training methods on real systems can be justified. Although the study dates back to 1992, the final negative answer to this query could still be considered as valid today.

The authors in [54] propose a NN hybrid controller (Fig. 4). The approach relies on an ideal controller containing a Recurrent-Neural-Network (RNN) uncertainty observer and a compensation controller to correct for the approximation error with respect to the ideal one. The authors tuned all parameters in the NN hybrid control system in the Lyapunov sense to guarantee stability. They then simulated the proposed control strategy with the same vehicle model used in [47]

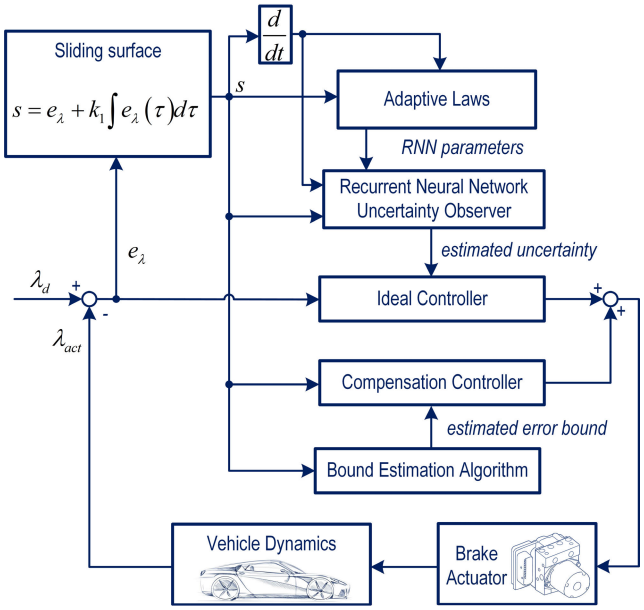

FIGURE 4. Neural network hybrid controller (adapted from [54]).

and compared the performance to a SMC design. In this simplified setting, the proposed design showed good tracking performance and robustness for various road conditions. In addition to this, the SMC outperforms the NN-based design in terms of braking distance. Several additional studies on NN applied to ABS can be found, for example, in [55] and [56].

D. PROPORTIONAL INTEGRAL DERIVATIVE (PID) CONTROLLERS

PID controllers are among the most used controllers in the industry. Fig. 5 details the general architecture of a PID controller as applied to a generic ABS. The proportional, integral, and derivative gains can be tuned to ensure that the desired system performance is being achieved around a desired operating point. These controllers, however, do not generally provide optimal control action and might show insufficient performance if the gains are poorly tuned (e.g., overshoots, oscillations, or cycling around the set-point) or when they are in the presence of constraint saturation.

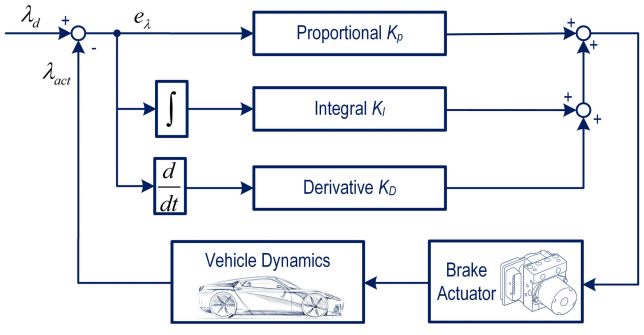

FIGURE 5. Generic ABS PID controller scheme.

PIDs are feedback controllers and do not rely on any knowledge of the system dynamics (only input-output behaviour is considered). This could be an advantage in general, but it can also lead to reactive behaviour. Additionally, PID controllers do not cope well enough with nonlinearities (e.g., actuator saturation) compared to another control techniques, require trade-offs between regulation and response time, do not react to changes in the process behaviour, and has a lag in the response to large disturbances. A further potential problem is that derivative term (D) can amplify process noise. Some of these issues can be mitigated. For example, low-pass filtering could be a solution to minimize the noise amplification when using the derivative term. The derivative action and the filtering, however, could have counter-action behaviour. Therefore, the amount of filtering should be limited, and low-noise instrumentation could be important [57]. Anti-wind-up techniques can be used to deal with actuator saturation.

In the context of ABS regulation problem, PID controllers could not achieve best performance under varying operating conditions due to the aforementioned issues. In this respect, several investigations evaluated the use of PID (either in simulation or with hardware-in-the-loop tests) and support the conclusion of the proposed paper [43], [44]. Nevertheless, several strategies are available and can effectively improve both performance and robustness of PID approach in ABS applications, as discussed below.

The differential band can be turned off with a relative loss of performance but with benefit for robustness increase. Gain scheduling based on vehicle velocity allows the controller to have high gains when the wheel dynamics is slow (higher speeds) and low gains as it becomes faster (as the speed decreases).

Augmenting the PI with sliding modes allows the controller to reduce its sensitivity to variation of road conditions (where oscillatory behaviour might occur). The authors in [58] discussed this last approach proposing a sliding-mode PI (SMPI). They implemented the design on a dSPACE processor board mounted on vehicle demonstrator equipped with EHB. They relied on standard wheel speed sensors and IMU for the state and parameter estimation (i.e., vehicle speed, brake lining friction coefficient, tire forces). The algorithms in closed-loop with the state estimator were tested. Additionally, to evaluate the advantages of the developed controllers over state of the art solutions, the also implemented a threshold-based algorithm. Both the properly tuned PI and the SMPI were found to be superior to threshold-based control on high- and low-friction cases. Additionally, SMPI leads to a 3-5% reduction in brake distance and a significant improvement in robustness compared to the PI.

Another option is to augment the PI controller (or any other feedback-only controller) with a feedforward term to improve the bandwidth of the regulation scheme. This idea has been investigated on a simple quarter car model in [59]. The authors used a cascaded wheel slip control strategy based on both wheel slip estimation and wheel

acceleration measurement. Additionally, they applied a set-point filter to smooth the response and improve control performance. This latest approach, however, is not always robust to sudden set point changes, which are commonly encountered in real ABS scenarios. Nonetheless, it was analytically demonstrated that the algorithm is able to globally and asymptotically stabilize the wheel slip around any prescribed set point.

Lastly, a mixed slip-deceleration control was introduced in [18]. The basic idea of this control approach is to select the regulated variable as a convex combination of the wheel slip and wheel deceleration. This strategy could be both powerful and flexible as it could reduce the detrimental effects of inaccurate wheel slip estimation, while avoiding the limitations of wheel acceleration control.

E. LQR CONTROL

Similar to PID controllers, linear quadratic regulators (LQR) are feedback controllers and are among the most popular optimal control approaches. Loosely speaking, they deal with the problem of finding a state-feedback control law for a given linear time-invariant (LTI) system to satisfy an optimality criterion.

The classical LQR feedback law is given by

$$u(t) = -R^{-1}B^T P^T x(t). \tag{1}$$

The control law is obtained by solving a quadratic optimization problem of the following form

$$\min \int_{t_0}^{\infty} \left(u(t)^T Ru(t) + x(t)^T Qx(t) \right) dt \tag{2}$$

where R is a positive-definite weighting matrix, Q is positive-semidefinite weighting matrix, and P is the solution of the algebraic Riccati equation associated with the system described by:

$$\dot{x}(t) = Ax(t) + Bu(t), x(t_0) = x_0 \tag{3}$$

where A and B are matrices of appropriate dimensions describing LTI system of wheel slip dynamics.

This method is generally suitable to control multi-input-multi-output (MIMO) systems. MIMO systems show strong couplings between states and, therefore, require tailored strategies to design the manoeuvre and achieve good performance. These systems often display significant nonlinearities or have non-minimum phase. Compared to PID controllers, LQR approaches require a model of the system to be controlled that might be complex and expensive to obtain.

Concerning ABS control, the explicit LQR approach taken by Johansen et al. is [60] of interest. Their work on the topic extends on the previous research discussed in [40]. The control design relies on local linearization and gain scheduling. The proposed control law contains no explicit friction model and relies on integral action, rather than adaptation, to eliminate a steady-state uncertainty. Following the LQR theory, they formulate the optimality condition as a standard quadratic cost function resulting in the optimal control input:

$$u(t) = -\underbrace{R^{-1}B^T(v)P^T}_{K(v)} x(t) \tag{4}$$

where P is the solution of the algebraic Riccati equation. The controller gain, namely $K(v)$, depends on the speed. Gain scheduling is achieved by letting

$$\frac{dQ(v)}{dv} > 0, \tag{5}$$

which reduces the gain as $v \rightarrow 0$. This is necessary to avoid instability due to the unmodeled dynamics tending to dominate as the velocity decreases and open loop wheel slip dynamics becomes faster. The authors proved that the control strategy is uniformly exponentially stable by using Lyapunov theory. The vehicle implementation, however, showed fundamental limitations on the achievable performance and maximum gain that could be tolerated before becoming unstable.

This issue has been handled in [61] by discretising and augmenting the controller with electro-mechanical brake-actuator dynamics and communication delays. The improved model is used for the synthesis of gain matrices at appropriate operating points, which are stored to provide an explicit piece-wise linear controller that incorporates actuator rate constraints. The controller is evaluated on various road conditions with different set-points. Several weak points are identified, for example, the initial transient response was not satisfactory due to significant modelling inaccuracies and noise in the low-slip region. Tests on wet tarmac partially covered with ice-simulating material revealed the controller is sensitive to friction coefficient variations and reacts with significant variability in the wheel slip error.

F. SLIDING MODE CONTROL

Sliding mode control (SMC) is a type of variable structure control system and it is characterized by a switching control action, as the system crosses a certain manifold in the state space, to force the state to reach, and thereafter to remain on a specified surface, called the sliding surface (Fig. 6). The system dynamics, when confined to the sliding surface, are termed as an ideal sliding motion and results in reduced-order dynamics with respect to the original plant. The reduction provides attractive advantages, such as insensitivity to parameter variations, matched uncertainties and disturbances.

Although sliding mode control was demonstrated as a powerful control method for ABS application [62]–[64], it has some disadvantages. In theory, the control action switching would occur at infinitely high frequency. As a result, the trajectories of the dynamic system are moving along the restricted sliding mode subspace. In practice, it is not possible to change the control infinitely fast because of time delays due to software and hardware limitations. Therefore, the sliding mode control action can lead to a high frequency oscillation, or chattering, that excites unmodelled dynamics. This could

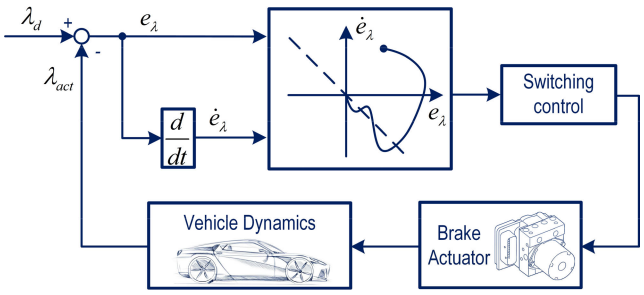

FIGURE 6. SMC ABS controller (adapted from [62]).

lead to energy loss, system instability, and excessive actuator wear [65], [66].

Different techniques were introduced to reduce chattering in ABS design. These methods smooth the discontinuous control law to achieve a trade-off between control-bandwidth and tracking precision. The simplest method is to replace the sign-function in the hitting control part with a saturation function or by other suitable continuous functions [67]. While these modifications are effective to reduce the chattering, these changes affect the tracking performance of the controller and do not ensure asymptotic stability. As an alternative, the authors of [68] proposed to replace the sign-function with a PI-like expression in a fixed neighbourhood around the switching surface. The authors of [69] proposed, instead, an improved continuous switching function that incorporates the state trajectory approach angle with respect to the sliding surface. In this way, the overall SMC guarantees asymptotic stability with a slight amount of system chattering. Harifi et al. in [70] used an integral switching surface, instead of sign function, to reduce chattering. In this case, however, the authors assume precise estimate on the bounds of the parametric uncertainties for the controller to work efficiently. Additionally, to suppress chattering conditional integrators [71] or offline optimization of the controller gains [72] have been also investigated.

SMC guarantees asymptotic stability in the presence of matched disturbances. In the case of unmatched disturbances only bounded stability can be guaranteed [73]. The authors of [74] analysed the robustness to uncertainties related to tire-road interaction of several SMC sliding surfaces for WSC in two-wheeled vehicles. The authors of [75] focused on these uncertainties, as well, by using a grey system modelling approach applied to SMC. This approach achieved enough reduction of wheel slip oscillations even in cases of significant road friction variation.

The authors of [76] proposed a SMC augmented with a Radial Basis Function (RBF) NN. The RBFNN comprises of a two-layer data processing structure, implementing a moving sliding surface. The adaptive rule is employed for online adjustment of the RBF weights by using the reaching condition of a specified sliding surface. Unlike conventional SMC, the dynamic sliding surface moves to the desired sliding surface from the initial condition, and thus the proposed design can achieve good tracking performance. The strategy can eliminate the reaching phase from conventional SMC, reduce chattering, and guarantee the system robustness during the whole control process. However, the *approach is limited by the previously discussed drawbacks of NN* in ABS. The authors of [77] developed a SMC using a second order switching surface for wheel slip control. Second-order SMC generalizes the basic sliding mode idea acting directly on the second-order time derivative of the sliding variable. This method, with respect to the first-order case, provides higher accuracy and generates continuous control actions while retaining the same robustness properties and a comparable design complexity. Additionally, by means of simulation, the method is proven to avoid complex stick-slip phenomena as no oscillations or overshoot take place during the transients. The authors claimed that it is not necessary to have precise values for the error signals for the controller to work. However, on a real system, the approach requires the first and second-order derivatives of the slip signal, which is already difficult to obtain reliably. Lastly, in contrast to first-order SMC, actuator dynamics cannot be considered.

The authors of [78] deployed a Pseudo-Sliding Mode approach for the design of a mixed slip-deceleration controller, well explained in [79], as well. The SMC framework allows to alleviate the control sensitivity to the actuator characteristic uncertainty, exhibited by the linear approach seen in [18]. The control architecture considers a more realistic, first-order LTI system to model the behaviour of electro-mechanical brakes resulting in nonlinear braking dynamics in contrast to [18], where a transfer function based on the linearized model description was employed. However, the approach relies on the Burckhardt-type tire model, that is, tire dynamics are not present, and the oversimplified simulation is not representative of the controller absolute performance. Nonetheless, it is appropriate for showing the superiority of SMC over PI in both dynamic performance and noise rejection.

The authors of [58] proposed an Integral Sliding Mode (ISM) controller and demonstrated that ISM provides compensation and estimation of the perturbations with less chattering compared to the SMPI. Compared to the switching threshold-based control, the approach reduces the braking distance by 31% and 25% with and without reference adaptation respectively, on the low friction road surface. The shortest stopping distance achieved by ISM control was 7% shorter than with PI and 2% shorter than SM (all with reference adaptation logic in the loop). Furthermore, the authors showed the robustness of the system by comparing the variations in braking distance of five subsequent tests: switching threshold-based causes deviation in 9% from the median value, while for the ISM case this was reduced up to 3%. The effectiveness of the reference adaptation algorithm results in a reduction in braking distance of up to 2% in comparison to the cases with pre-set reference wheel slip. This confirms the hypothesis that, during the emergency braking, the optimal area of the λ-F_x friction curve can deviate from its initial value and emphasizes the importance of reference adaptation.

G. CLASSICAL ROBUST CONTROL

H_∞ control designs are robust control approaches. A robust control design explicitly deals with uncertainty to achieve robust performance and stability in the presence of bounded modelling errors. In contrast with an adaptive control, robust control is designed to work in a static way, rather than adapting to measurements of variations. An H_∞ controller is designed through optimizing the infinite norm of a performance index in H_∞ space. By minimizing the sensitivity of a system over its frequency spectrum, this design can guarantee that the system will not greatly deviate from expected trajectories in the presence of disturbances. Finding an optimal H_∞ controller is often both numerically and theoretically complicated, as discussed in [80].

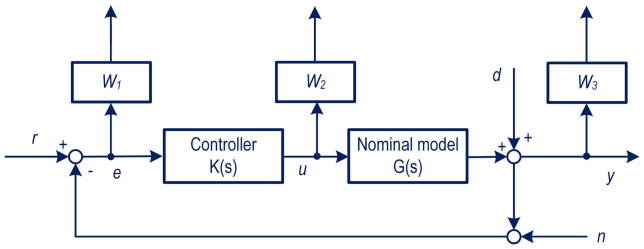

FIGURE 7. Design method based on mixed sensitivity (adapted from [81]).

Fig. 7 shows a general scheme of the approach, where r, e, n, d and y are the reference input, tracking error, measurement noise, disturbance input and system output, respectively. W_1, W_2 and W_3 are the weight functions of the performance of the system, output constraints of the controller and the system robustness, respectively. The H_∞ mixed sensitivity control consists in choosing the weighting function W_1, W_2 and W_3 in the frequency domain such that condition (6) is satisfied, where Q, R, T are the transfer functions from r to e, u and y respectively.

$$\left\| \begin{matrix} W_1 Q \\ W_2 R \\ W_3 T \end{matrix} \right\|_\infty \leq 1 \tag{6}$$

The authors in [81] proposed H_∞ robust controllers designed via a simplified ABS mathematical model by mixed sensitivity method. They design the controller according to the nominal plant model to keep the controlled system steady and the H_∞ norm of the sensitivity function small. The controller is evaluated in simulation environment with a quarter car model. The manoeuvre represents friction transition such as a μ-transition, and satisfactory performance has been achieved.

In the context of robust control, a possible option is to use Linear Matrix Inequalities (LMIs) to approximate and solve robust control problems in a more tractable form. In the context of ABS designs, the authors of [82] proposed a robust control method using a Linear Parameter Varying (LPV) system representation and used LMIs to derive conditions for the existence of the state-feedback controller. They used as plant model a quarter car model with Pacejka's Magic Formula (MF).

The authors of [83] relied on a similar LMI technique to avoid the chattering effect in the design of a SMC controller. In particular, the work considers the system unmatched uncertainties in the design of ABS system by employing LMIs to design a stable sliding surface. Compared to the approaches described in the SMC Section, this method incorporates uncertainties in the design phase. The proposed controller has been investigated on a quarter car model showing that robust stabilisation and chattering reduction can be achieved.

H. MODEL PREDICTIVE CONTROL

Similar to optimal control, model predictive control (MPC) relies on optimization to find the optimal control input to apply to the plant. In contrast to LQR, MPC solves online a *constrained* Optimal Control Problem (OCP) over a finite time window, called prediction horizon. An example of general OCP is described below:

$$\begin{aligned} &\min \int_{t_0}^{t_0+T_p} \Big[\underbrace{\left\| y(t) - y_{ref}(t) \right\|_Q^2 + \left\| u(t) - u_{ref}(t) \right\|_R^2 + \left\| y(t_0+T_p) - y_{ref}(t_0+T_p) \right\|_P^2}_{J} \Big] \\ &x(t_0) = \tilde{x}_0 \quad \text{initial conditions} \\ &\dot{x}(t) = f(x(t), u(t)) \quad \text{plant dynamics} \\ &y(t) = g(x(t), u(t)) \quad \text{output mapping} \\ &x_{\min} \leq x(t) \leq= x_{\max} \quad \text{state constraint} \\ &u_{\min} \leq u(t) \leq= u_{\max} \quad \text{actuator constraint} \end{aligned} \tag{7}$$

The solution of the OCP is the result of minimizing the cost function J over the horizon T_p. Q and P are positive semidefinite weight matrices penalizing the deviations of the outputs y from their reference values y_{ref} and R is positive definite weight matrix penalizing the deviations of the inputs u from their reference values u_{ref}. The weight matrices are usually tuning parameters with a physical interpretation.

In contrast to LQR, MPC works over a *finite* time horizon to make the constrained optimization problem tractable online (it would be computationally impossible to solve a constrained infinite horizon problem with an infinite amount of decision variables and constraints). MPC formulates a parametric optimization problem, in which the parameters are the current states $\tilde{x}_0$ of the system. Based on the current system states, by using a dynamic model to describe the system (plant dynamics), the controller computes a sequence of optimal control commands that minimizes J and satisfies the state and actuator constraints. Only the first element of the obtained control sequence is applied to the plant, according to the receding horizon principle. Every time the controller receives new measurements from the plant the process is repeated. The MPC problem formulation can be either convex or nonconvex and can accommodate both linear or nonlinear plant models and constraints. The general structure of a discrete time model predictive controller for wheel slip control is shown in Fig. 8.

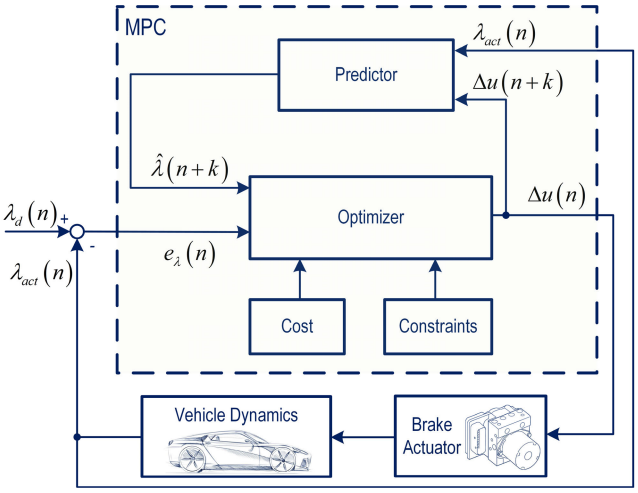

FIGURE 8. General structure of model predictive control.

MPC has the advantages of incorporating constraints and accurately predicting (if an accurate model of the system is available) the change of system dynamics along the prediction horizon. Robust MPC [84] implementations are also possible (and involved the use of constraint-tightening methods [85], tubes [86], or chance-constraints [87]). The main drawback of MPC is related to the computational requirements for online computation that could make the implementation of the controller for real-time applications challenging or even impossible. For linear systems and polytopic constraints, the MPC problem reduces to a quadratic programming problem, which can be solved efficiently. The computation load substantially increases when dealing with nonlinear systems and non-convex constraints. Efficient online solvers (such as IPOpt [88] and QPOASES [89]) have been developed for these formulations, but they only provide convergence to local minima. In addition to this, the computation time is often unpredictable, which could be a problem for safety critical real-time applications.

Nonetheless, there have been attempts in using MPC for ABS applications. Anwar et al., reiterating on what was proposed for yaw dynamics control in [90], a generalized predictive ABS control based on a Controlled Auto Regressive Integrated Moving Average model [91].

The authors of [92] proposed the Independent Model Generalized Predictive (IMGPC) control introduced by Rossiter [93] for ABS control. The control system is tested on a simple linearized quarter-car model (with an unspecified tire model) in the presence of severe disturbances and noise. Their results showed that, with a long prediction horizon (500 samples), MPC performed better than LQR in terms of noise and disturbance rejection. The online computational load is not mentioned in these studies.

The authors of [94] showed an optimization-based brake torque control law. The prediction model is obtained from a quarter car model equipped with Dugoff non-linear tire model augmented with a first-order transfer function for the tire dynamics and first order actuator dynamics (EMB). To increase the robustness of the controller, they augmented the state with the integral of the wheel slip. They also analysed the effect of the continuous time prediction horizon on the tracking error. They found that, as the prediction horizon increases the tracking error decreases up to a point, in which the control energy becomes oscillatory and chattering occurs. The proposed controller demonstrates better performance compared to the controller with the SMC algorithm from [67] on dry and slippery roads including uncertainty levels of the total vehicle mass and the friction coefficient.

The authors of [95] took a step forward from simulation to HIL experiments. They proposed a distributed wheel-slip controller using MPC using a longitudinal vehicle model (a quarter car model) as prediction model assuming that each wheel remains on the same road surface. The predefined longitudinal slip stiffness is used to compute the longitudinal force. Tire relaxation dynamics is included in MPC formulation. The constrained optimal control problem is solved online with primal-dual method of the Hildreth's quadratic programming algorithm. The controller evaluation is performed on high-, mid-, and low μ surfaces and for each of them the wheel slip error is found to be relatively small and oscillations, although present, are confined. The main limitation is that longitudinal slip stiffness is predefined for a given road surface.

The investigation [96] proposed the design of linear and nonlinear model predictive controllers (solved using Forces Pro [97]) incorporating a predefined MF tire model for wheel slip control using friction brake system and near-wheel electric motors. The simulation-based assessment is performed using an IPG/Carmaker vehicle model for various road surfaces and μ-split braking showing accurate tracking performance and robustness against tire-road friction coefficient uncertainty. During μ variation a notable offset from the reference wheel slip is observed due to the predefined MF parameters, which requires adaptation of the internal model.

To overcome real-time capability issue related to MPC, the usage of explicit nonlinear MPC could be potential solution assuming availability of a high-fidelity model on the design stage. The authors of [98] proposed an original explicit nonlinear MPC solution evaluated in EHB HIL test bench and IPG/Carmaker model with first-order transient tire dynamics, and compared to PID ABS. This solution outperforms PID ABS resulting in 11.4% decrease in the brake distance for low μ conditions. The needs to update the predefined tire model in the controller can be considered as the limitation similar to the previous research.

I. DISCUSSION

Based on the state of the art, the following conclusions can be derived:

- Threshold-based (rule-based) algorithms compose the vast majority of ABS controllers found on today's vehicles but are time-consuming and supplier-dependent to tune due to their heuristic nature and a large list of

tuning parameters. Additionally, considering the recent improvements in actuator technology and trend towards the coordinated chassis control, their potential is significantly underused.

- Controllers based on fuzzy logic suffer from similar issues, such as the large number of tuning parameters, membership functions, and rules, which increase exponentially with the complexity of the application. In general, fuzzy approaches are good for those processes that, although containing uncertainty, do not present the large variability band intrinsic to the ABS regulation problem. For a controller addressing everyday situations in accordance with the ABS safety requirements, thousands of rules would be needed, and it would be extremely inconvenient, if even possible, to tune them. This conclusion is contradictory to the conclusions performed in the survey in 2011 [35].
- Neural networks approaches require a very large set of training data to achieve adequate performance and robustness. For the WSC tasks, this is extremely consuming in terms of time and resources.
- PIDs struggle with nonlinearities and can become unstable if countermeasures are not in place (e.g., anti-windup strategies).
- LQR methods are feedback controllers sensitive to modelling errors and do not accommodate any feedforward action that could be beneficial for ABS applications.
- SMC demonstrates better performance and robustness than the PID. SMCs combined with methods that allow to reduce chattering (e.g., the ISMC) are the best reactive wheel slip controllers in this regard. SMCs approaches, however, are still rarely validated by real-world experiments. Finally, similar to LQR, SMC is a feedback technique and adding feedforward action is nontrivial, limiting the performance of the controller.
- Classical robust control approaches allow to deal with disturbances and noise by design; however, the performance evaluation of ABS controllers using these approaches is limited compared to other methods.
- Model predictive control is a promising approach that offers space for improvements in terms of performance and robustness with respect to state of the art controllers. Compared to other designs, MPC also proposes a modular framework that it is intuitive to understand and maintain. The main limitation of MPC is related to the computational burden, especially if the control problem is nonconvex. Nevertheless, the advance in microcontrollers processing power, solvers for nonconvex optimization, and the drive towards a model-based integrated chassis control will mitigate this drawback.
- Several control methods such as iterative learning [99], backstepping [100], nonlinear feedback control [101] and flatness-based [102] were not considered in this paper due to limited studies for WSC application.

TABLE 1. Summary of control strategies.

	Tracking performance	Realization difficulty	Robustness	Amount of parameters	Easy to tune	Computational load	Adaptability	Implementation intensity
RB	◔	◔	◕	●	○	○	◕	●
FLC	○	◑	◑	◕	◔	◔	◔	◔
NNC	◔	◑	◔	◕	◔	◑	◔	◔
PID	◕	○	◑	○	●	○	◔	◑
LQR	◕	◑	◑	◔	◑	◑	◑	◔
SMC	◕	◕	◕	◑	◑	◑	●	◑
Robust	◑	◕	●	◕	◔	◕	◑	○
MPC	●	●	◕	◑	◕	●	◕	◔

● Highest ◕ High ◑ Average ◔ Low ○ Lowest

- Lastly, one of the weak-investigated directions and in the starting point of the research in WSC is the usage of reinforcement learning [103], [104] and deep learning.

A summary of the analysed control strategies is presented in the Table 1 using Harvey Balls.

Based on the considerations above, MPC should be further investigated by the research community to understand its full capabilities. This motivates the case study proposed in Section IV. Current trends related to automated driving resulting in the usage of on-board high-performance computational processors that the major drawback of an MPC approach, computational effort, is decreasing in importance and could be outweighed by its performance benefits.

III. ABS TESTING AND KEY PERFORMANCE INDICATORS

To assess the controller's performance, its behaviour should be compared with the state of the art solutions. Demonstrating the stability of the ABS controller is also a key point that remains unsolved. Classical stability theory to validate such complex designs is extremely difficult to apply. Traditional approaches can only prove closed-loop stability of the system model used in the analysis and not the real plant. In theory, this would require developing high-fidelity models of the system in differential equation forms. In practice, deriving these models is too difficult.

To overcome these issues, a comprehensive set of manoeuvres should be used to empirically demonstrate the stability of the developed design. Moreover, a set of key performance indicators (KPIs) is proposed to analyse and interpret the results. Selecting the right manoeuvres and KPIs is not trivial and requires extensive evaluation of regulations and technical documents. The aim of this section is to summarize this research to simplify the future design evaluations. The proposed manoeuvres and KPIs are discussed below.

A. ABS TESTING SCENARIOS

The goal of the manoeuvre selection is to span all possible conditions that might be encountered on the road.

Attention is therefore focused on identifying a restricted set of manoeuvres that is representative of a much larger set of possible conditions. Braking scenarios were chosen based on the guidelines given by the United Nations in Regulation 13 (E/ECE/- TRANS/505/Rev.1/Add.12/Rev.8. 3. Regulation No. 13) and Toyota's internal knowledge.

The eight selected manoeuvres, reported in Table 2, belongs to three major groups:

TABLE 2. ABS straight-line test scenarios.

	Initial velocity	Avg. Friction coefficient *	Exit velocity	Surface layout	Extra
High friction	130kph	1	5	Smooth	
Mid friction	90kph	0.7	5	Smooth	
Low friction	40kph	0.3	1	Smooth	
mu-jump	120 kph	1.1 → 0.58	70	Smooth	jump@100kph
mu-jump	>50 kph	0.8 →0.3	30	Smooth	jump@40
mu-jump	70	0.3 → 0.8	20	Smooth	jump@55
Rough road	70	0.7	0	Wet red bricks	
Rough road	40	0.3	0	Wet Belgian	

Braking on smooth roads – Three manoeuvres are targeted at evaluating the performance gain on smooth roads with constant friction conditions. Three friction levels are selected, associated with dry asphalt, wet asphalt and packed snow. The initial speed for each of three decelerations is chosen for relatable domains' speed limits (e.g. high-way, freeway, etc.) and advisable maximum speed associated with the friction condition.

Friction transition – The three μ-transition manoeuvres (performed on smooth roads) are specifically intended for evaluation of the controller transient behaviour. Friction transitions are commonly found on everyday roads and it is therefore key for the controller to be fast adapting and robust to them. To assess the controller behaviour in relation to transient conditions, two friction transitions in which the friction coefficient drops and one in which it raises are typically simulated. The speed at which the transition happens can be selected based on typical operational conditions for a given vehicle.

Braking on rough roads – Two last manoeuvres are performed on rough surface. The objective is to quantify and compare eventual performance degradation when injecting high-noise levels in the sensed signals. Road irregularities, in fact, are transmitted through the vehicle and cause variable band noise on the sensor measurement. As frequency and amplitude are dependent on the road shape, it is usually difficult to filter the disturbance out.

Extra test procedures related to μ-split conditions are not considered in this paper.

B. KEY PERFORMANCE INDICATORS

Different KPI sets have been selected for each of three groups of manoeuvres.

Steady state and transient performances, as well as human factors and actuator wear, are evaluated on smooth roads by the following KPIs:

ABS Index of Performance(*ABSIP*) – this KPI compares the braking distance achieved by the specific controller to that of the case in which ABS is not present. The returned value, a brake distance reduction percentage, gives a first rough idea of how effective the controller is throughout the braking manoeuvre:

$$ABSIP = \frac{d_{ABS}}{d_{skid}} \tag{8}$$

Brake Distance(*BD*) – the KPI is calculated as the velocity integral from the moment, at which the brake pedal is first pressed t_i, to that, in which the vehicle speed equals to the exit velocity t_f reported in Table 2. The aim is also to compare overall braking performance but this time with an absolute brake distance:

$$BD = \int_{t_i}^{t_f} V_x dt \tag{9}$$

Mean Fully Developed Deceleration(*MFDD*) – this KPI is simply the mean longitudinal acceleration, $\bar{a}_x$, calculated in a time interval that goes from 90% to 5% of the vehicle speed V_0 at the beginning of the braking. The MFDD is specifically designed for assessment the vehicle deceleration performance throughout the entire ABS activation time.

$$MFDD = [\bar{a}_x]_{0.05V_0}^{0.9V_0} \tag{10}$$

ABS efficiency(η_{ABS}) – this KPI is the ratio of mean longitudinal acceleration to its theoretical maximum (product between average friction coefficient $\bar{\mu}$ and gravitational constant g). $\bar{a}_x$ is calculated from when the vehicle velocity equals 80% of its initial speed to when the vehicle is at 5% of its initial speed. This KPI is specifically designed for assessment of steady state deceleration performance. The steady state covers the interval after the initial weight transfer up to the point at which the ABS switched to its low speed mode and pressure modulation is stopped.

$$\eta_{ABS} = \frac{[\bar{a}_x]_{0.05V_0}^{0.8V_0}}{\bar{\mu} g} \tag{11}$$

Peak to Peak (*PTP* or ω_{peak}) – KPI quantifies the agility of the controller in transient conditions. This is done by focusing only on the first control cycle after ABS activation and it is calculated in a similar fashion to a normalized slip error except that the vehicle velocity is not needed for the calculation and thus simulation results can be replicated more easily in real life. $\omega_{\max,k}$ is the wheel angular velocity at either ABS activation or friction transition. $\omega_{opt,k}$, on the other hand, is the optimal wheel speed obtained from the tire model. An illustration of these two wheel speeds is shown in Fig. 9.

$$\begin{aligned} \omega_{peak} &= \sum_k \frac{\omega_{\max,k} - \omega_{opt,k}}{\omega_{\max,k}} \\ k &= [FL, FR] \wedge [RL, RR] \end{aligned} \tag{12}$$

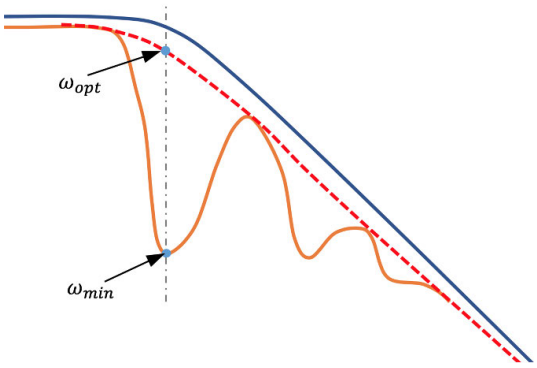

FIGURE 9. Illustration of the Peak to Peak KPI (PTP).

Integral Time-weighted Average of the longitudinal jerk ($ITAE_{J_x}$) – KPI aims at characterizing driving comfort. A negative influence on the driver's perception during ABS braking occurs owing to fluctuations in the realized brake force, which produces oscillations in the vehicle deceleration. Here, the lower the vehicle jerk, the better the comfort characteristics provided by the ABS are. Weighting the average with time, corresponds to taking the area between the jerk signal j_x and zero (an ideal value). Additionally, taking the integral has the important advantage of filtering out outliers and spikes (commonly originated by differentiating a noisy signal as their contribution to the area is zero). In this way the signal does not require complex filtering.

$$ITAE_{J_x} = \int_{t_i}^{t_f} t\,|j_x|\,dt \tag{13}$$

Integral torque variation – Actuator wear ($IACA_{T_b}$) – KPI calculates how much torque variation is prescribed by the controller. This is important for a first evaluation of potential issues related to actuator wear. Large torque variation can lead to premature degradation of both brake components and valves. Estimating how much this number should be considered as critical is outside the scope of the proposed work.

$$\begin{aligned} IACA_{T_b} &= \int_{t_i}^{t_f} \sum\nolimits_k \left|\dot{T}_{b,k}\right| dt \\ k &= [FL, FR, RL, RR] \end{aligned} \tag{14}$$

Integral Pitch Variation (IPV) – this KPI relates to the human factors. The driver capability to estimate distance is significantly deteriorated in the presence of excessive vehicle pitch angle φ [105]. Therefore, it is desirable for an ABS to be as smooth as possible during the control action. IPV is mostly relevant on high friction surfaces due to larger load transfer causing high variation of pitch angle.

$$IPV = \int_{t_i}^{t_f} |\varphi|\,dt \tag{15}$$

KPIs used for the friction transitions scenarios are focused on analysing the controller behaviour after μ-transition. Here two key aspects are transient performance and lateral stability. The indices are as follows:

Recovery time (T_{rec}) – – KPI quantifies how much time is taken by the controller to recover from the friction transition and go back to steady state conditions. The counter is started when the front wheels first experience the change in surface condition and runs until the longitudinal acceleration is inside a certain band. The band is identified as $\pm 5\%$ of the mean longitudinal acceleration$\bar{a}_x$ after the transition.

$$T_{rec} = [t]_{i,jump}^{\pm 5\%\bar{a}_x} \tag{16}$$

Peak to peak at friction transition($\omega_{peak,jump}$) – – the focus is only on the first control cycle after the friction transition. Generally, the depth of the first cycle significantly affects the ABS performance, and it is therefore highly important to try minimizing this specific aspect. The metric is of particular interest (i) for lower friction coefficients where the cycle takes significantly more time, and (ii) for under-braking, to demonstrate the recovery from the unstable part of the λ-F_x friction curve. It is calculated in the same way as for ω_{peak}.

Mean deceleration at friction transition ($\bar{a}_{x,jump}$) – – KPI targeted at quantifying the overall deceleration performance during the friction transitions. The calculation starts 0.2s before the front wheels experience the change in friction and ends 1s after the rear wheels have performed the transition.

$$\bar{a}_{x,jump} = \int_{t_{i,jump}}^{t_{f,jump}+1} a_x dt \tag{17}$$

Maximum yaw rate at friction transition ($\dot{\psi}_{\max}$) – – KPI aims at quantifying the vehicle stability during the friction μ- transition manoeuvre. It is not uncommon for a vehicle experiencing a sudden change in friction to exhibit some yawing. Yaw angles are usually not high since the wheel pairs undergo the friction transition at the same time. Nonetheless, the velocity at which the vehicle rotate should be contained in order to allow the driver to counter steer. The usual threshold for acceptability is set around a value of $1 - 1.5$ deg/s.

$$\dot{\psi}_{\max} = \max\left[\dot{\psi}\right]_{i,jump}^{f,jump} \tag{18}$$

For rough roads, the indicators are the same as that introduced for smooth roads.

For the evaluation of μ-*split testing,* brake distance, vehicle deceleration, maximum yaw rate and corrective steering angle are typically used.

IV. CASE STUDY: A NONLINEAR MODEL PREDICTIVE CONTROL ABS DESIGN

Motivated by the conclusions in Section II.I, the proposed case study investigates the use of nonlinear model predictive control (NMPC) for ABS applications. The paper goal is to show the potential of this technique compared to the current industry-used threshold-based logic in the scenarios and with

the KPIs discussed in the previous section. First, to use NMPC, a model that accurately describes the dynamics of the system needs to be defined:

$$\begin{aligned}
\dot{\lambda}_{FL} &= \frac{1}{V_x}\left[\frac{r_w}{I_w}\left(dT^{cmd}_{b,FL}\tau + T_{b,FL} - F_{x,FL}r_w\right) - \frac{1-\lambda_{FL}}{0.5m_f + m_s a_x h/2L}\right] \\
\dot{\lambda}_{FR} &= \frac{1}{V_x}\left[\frac{r_w}{I_w}\left(dT^{cmd}_{b,FR}\tau + T_{b,FR} - F_{x,FR}r_w\right) - \frac{1-\lambda_{FR}}{0.5m_f + m_s a_x h/2L}\right] \\
\dot{\lambda}_{RL} &= \frac{1}{V_x}\left[\frac{r_w}{I_w}\left(dT^{cmd}_{b,RL}\tau + T_{b,RL} - F_{x,RL}r_w\right) - \frac{1-\lambda_{RL}}{0.5m_r - m_s a_x h2L}\right] \\
\dot{\lambda}_{RR} &= \frac{1}{V_x}\left[\frac{r_w}{I_w}\left(dT^{cmd}_{b,RR}\tau + T_{b,RR} - F_{x,RR}r_w\right) - \frac{1-\lambda_{RR}}{0.5m_r - m_s a_x h/2L}\right] \\
\dot{T}_{b,FL} &= dT_{b,FL} \\
\dot{T}_{b,FR} &= dT_{b,FR} \\
\dot{T}_{b,RL} &= dT_{b,RL} \\
\dot{T}_{b,RR} &= dT_{b,RR} \\
a_x &= \left(F_{x,FL} + F_{x,FR} + F_{x,RL} + F_{x,RR}\right)/m_s
\end{aligned} \tag{19}$$

where $F_{x,ij}$ is the longitudinal tire force, a_x is the longitudinal acceleration, V_x is the chassis velocity, I_w is the wheel inertia, L is the the wheel base, r_w is the effective rolling radius, m_s is the sprung mass, m_f and m_r are the portions of the total mass resting on the front and rear axles, respectively. The first four equations describe the wheel slip dynamics of each wheels λ_{ij}. Additional four augmentation equations $T_{b,ij}$ allow the MPC to control the torque rate $dT_{b,ij}$ instead of the brake torque. Finally, the last equation describes the chassis longitudinal dynamics. The model also considers the effects related to the brake actuator dynamics and longitudinal weight transfer. In particular, the EHB system behaviour is represented by a first-order dynamics with the time constant τ, and the longitudinal weight transfer is approximated by its static part. Finally, online wheel force data is used (obtained from the load sensing bearings including accuracy and noise level [31]) to formulate a complete description of the tire dynamics. The state vector is given by the following:

$$x = \left[\lambda_{FL}, \lambda_{FR}, \lambda_{RL}, \lambda_{RR}, T_{b,FL}, T_{b,FR}, T_{b,RL}, T_{b,RR}, V_x\right]^T \tag{20}$$

The control commands (i.e., the brake torque rates, $dT^{cmd}_{b,ij}$) can be obtained by solving the associated optimal control problem that includes the model described above as the prediction model and the constraints discussed below.

Table 3 summarizes the state and input constraints. These bounds were selected according to the following reasons:

TABLE 3. State and input bounds.

Variable	Units	Lower-bound	Upper-bound
T_b (front)	Nm	0	3500
T_b (rear)	Nm	0	1700
λ	-	0	1
V_x	m/s	0	53
$\dot{T}_b$ (front)	Nm/s	-35000	42000
$\dot{T}_b$ (rear)	Nm/s	-35000	35000

TABLE 4. Important controller settings.

VARIABLE	Units	Value
Prediction horizon T_p	s	0.100
Sampling time T_s	s	0.005
Controller frequency f_{ctrl}	Hz	250

- The lower bound for the chassis velocity is set to 0 to prevent the vehicle from going backwards, while the upper-bound is selected equal to the vehicle's maximum speed.
- The brake torque lower bound is 0 Nm given that negative numbers would mean that a driving torque is applied. The upper bound is the system's maximum capability. Given the different sizing of front and rear brakes, two values are listed in Table 3.
- Given that the EHB pressure increase rate is approximately 1300 bar/s and assuming the system is 30% slower in damping pressure based on the previous investigations [106], the torque rate is limited for the considered vehicle. For stability reasons it is advisable for rear wheels to follow the front ones in the event of a lock up. Hence, the rear-pressure increase rate of the rear axle is lowered.

The tool used as modelling environment to define the optimal control problem is ACADO Toolkit. ACADO is an open-source software environment for dynamic optimization which supports self-contained C code [107]. Its most appealing features is the task scheduling of the Real Time Iteration (RTI) scheme which splits one iteration into two phases: a preparation phase, where the NLP is linearized, discretized and condensed; and a feedback phase, where the condensed QP is solved. Since operations are parametric in the initial state x_0, the preparation can be done offline. In this way, the solver can achieve real-time performance within the milli- or micro-seconds range (depending on the application) [89]. The NMPC problem reduces to a dense QP that ACADO solves by using qpOASES [108]. Table 4 reports the most relevant settings of the solver.

As mentioned, NMPC is the key element of the proposed ABS formulation. Nevertheless, other components are also important for the correct behaviour of the design under discussion. Fig. 10 provides an overview of the overall control structure.

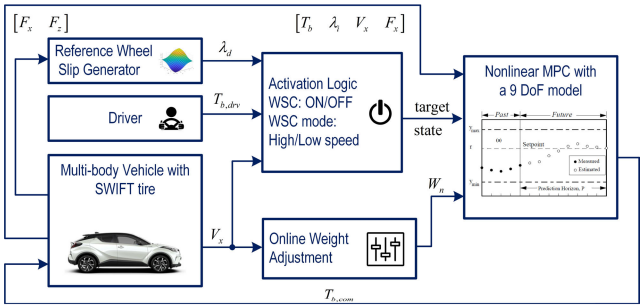

FIGURE 10. Proposed ABS controller scheme.

TABLE 5. Weight scheduling.

Weight	Values		
	ABS off	ABS on	ABS low speed
$W_{\lambda f}$	0	5e+8	0
$W_{\lambda r}$	0	3.5e+7	0
W_{Tbf}	50	0	50
W_{Tbr}	50	0	50
W_{dTbf}	1e-5	$f_f(V_x)$	5e+5
W_{dTbr}	5e-5	$f_r(V_x)$	5e+5
W_{Vx}	0	0	0

The *reference wheel slip generator* reads the longitudinal and normal forces ($F_{x,ij}$ and $F_{z,ij}$, respectively) at each time step and, after calculating the friction coefficient μ_{ij}, outputs the reference wheel slips λ_d based on a 3D-map obtained from tire testing conducted by Toyota. The slip target, together with other signals coming from the vehicle and driver subsystems, are then passed to the activation logic.

The *activation logic* is responsible for cycling through three possible controller states: (i) ABS Off, (ii) ABS On, and (iii) ABS On - Low Speed. A state machine selects the controller's mode and target state. Whenever the ABS is inactive the NMPC acts as a driver brake request follower. Activation of the ABS controller is triggered based on some predefined wheel deceleration thresholds for front and rear wheel pairs. In a range from 1 m/s to V_{max}, the ABS operates as a slip target follower. Below 1 m/s, where the wheel dynamics is too unstable to control, the brake torque is kept constant to avoid any under-braking.

Based on the selected control mode, the *online weight adjustment logic* selects the entries of the weight matrices Q, P and R (R is equal to Q). In this formulation Q and P are diagonal matrices containing state weights and control weights respectively (Table 5). When the driver is in control (ABS off), the MPC is forced to track the driver demand using the weight entries from Table 5.

When the ABS is working in normal mode, the controller acts as a wheel slip reference tracker. Since the vehicle velocity acts as a time-scale factor for the slip dynamics, cost weights are defined to track the slip target with an increasingly larger control effort to cope with the progressively higher slip frequency. Weight functions $f_f(V_x)$ and $f_r(V_x)$ are two monotonically decreasing functions.

In low speed ABS mode, the brake torque applied to each wheel is kept constant to prevent any unwanted under-braking. To achieve it, the brake torques and rates are being prioritized.

The NMPC receives the current state, target state, online force measurements and cost weights to calculate the optimal actuator commands, that are, the brake torques. The optimized brake torques are then used as the target for the low-level ABS controller, which directly operates the hydraulic unit. Individual wheel pressures are then applied to the vehicle to close the control loop.

The performance of the proposed NMPC controller was compared to an industry-used threshold-based controller. Fig. 11 shows the high-end simulation setup used for evaluation.

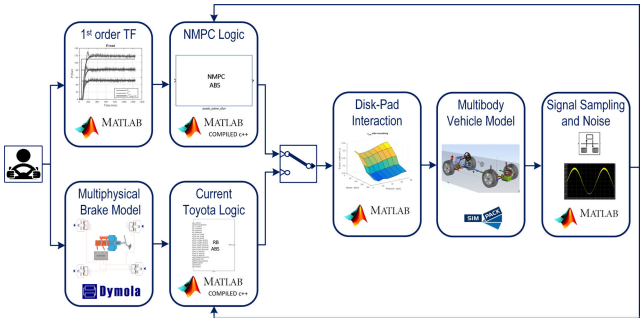

FIGURE 11. Vehicle co-simulation layout.

Each of the main vehicle subsystems was developed in the appropriate simulation tool, namely, MATLAB/Simulink for the controller, Simpack multi-body software for the vehicle model, Dymola multi-physics simulation software for the brake system and Delft-Tyre MF-SWIFT (Short Wavelength Intermediate Frequency Tire) model for tire behaviour. The models were then interconnected to replicate full vehicle behaviour.

The vehicle model was validated against a large set of experimental data collected by Toyota. The compliance of the flexible bodies were measured on dedicated test benches. The hydraulics of the brake system behaviour was replicated following a multi-physics approach. The pad-disc friction coefficient was modelled by a look-up table, whose values depended on vehicle velocity, pressure and temperature. The relationship was obtained by analysing test data for friction coefficient measurement according to the SAE J2522 standard (known as AK Master). More advanced approaches for pad-disc interaction can be based on dynamical models, e.g. [109], [110], or finite element modelling, e.g. [111]–[113].

Finally, to reproduce sensor behaviour, the information coming from the simulation is altered to match the signal quality.

TABLE 6. Friction transition dry-wet – KPI values.

KPI	Units	Threshold-based	NMPC
$\overline{a}_{x,jump}$	m/s^2	2.52	4.38
T_{rec}	s	0.580	0.360
$MDFF$	m/s^2	4.07	5.88
ω_{peak} (front)	%	66.60	14.67
ω_{peak} (rear)	%	26.77	13.35
$\dot{\psi}_{\max}$	deg/s	1.83	0.93

Eight ABS braking scenarios were evaluated according to the test manoeuvres presented in Section III. In particular, the results are presented for (i) friction transition from dry-wet, (ii) smooth dry asphalt, and (iii) packed snow. A full analysis for (ii) and a spider plot summarizing the findings for (i) – (iii) are presented. More details regarding the performed analysis is given in [114].

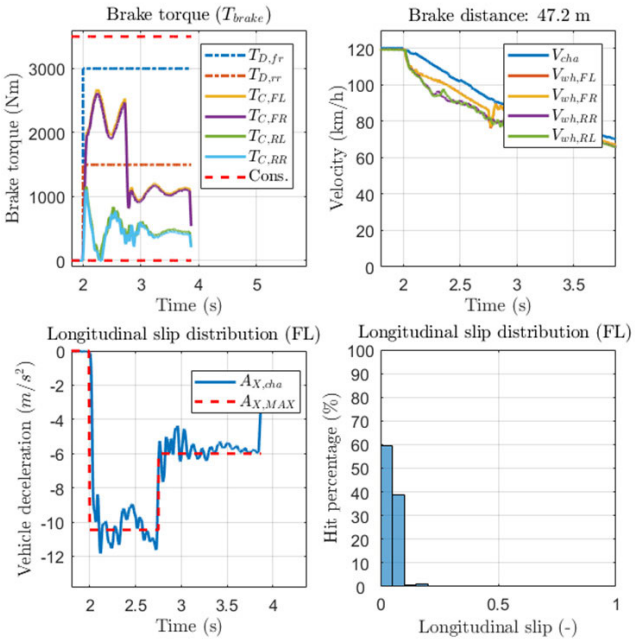

FIGURE 12. Friction transition dry-wet time histories – NMPC.

Fig. 12 presents the results for friction transition. As the figure shows, once the controller becomes active, the front brake torques increase to take advantage of the longitudinal weight transfer, while rear ones decrease. When the vehicle starts to pitch back, the behaviour is reversed. Steady state would eventually be reached; however, at 2.5 s the friction transition occurs, and brake torques promptly reduce. The predictive behaviour of the NMPC controller allows (i) the system to limit the under-braking and (ii) the torques converge to their optimal value net of vehicle pitching.

The comparison between the wheel speeds and vehicle speed (Fig. 12) highlights the absence of the typical threshold-based ABS control cycles (i.e., increase, decrease, and hold pressure). The longitudinal slip distribution graph

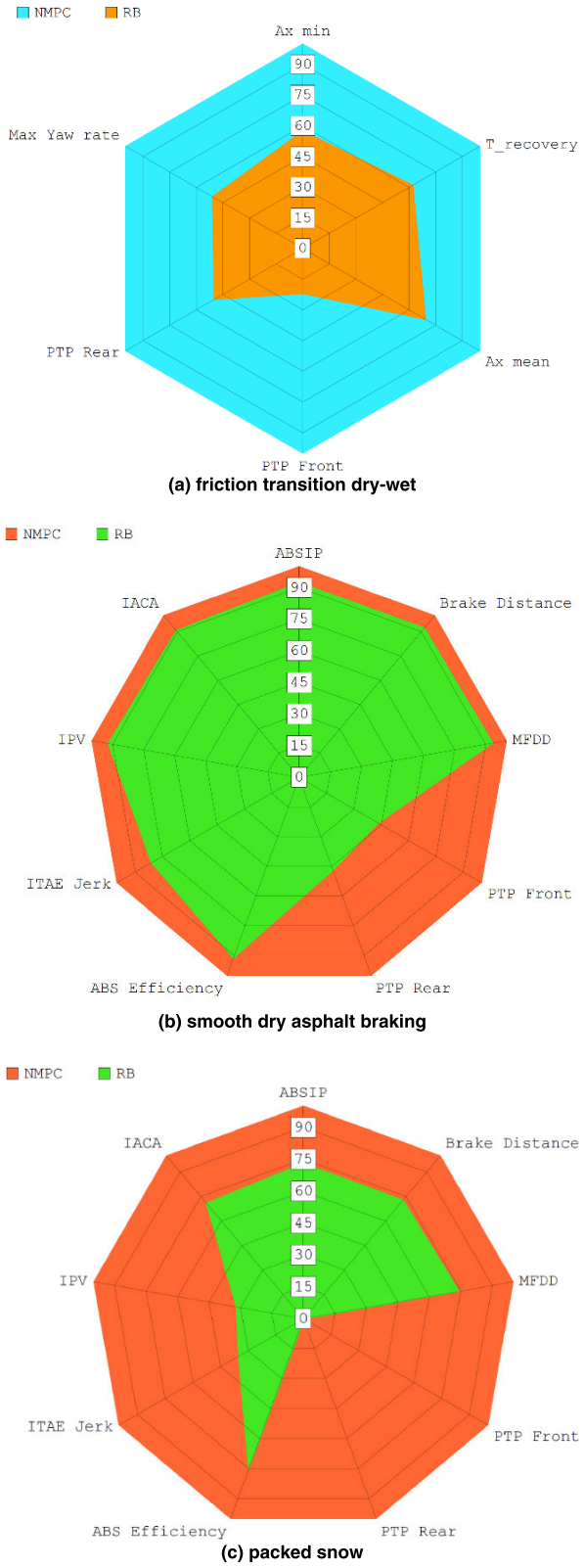

FIGURE 13. KPIs for straight-line braking.

of the front-left wheel (bottom plots) shows how the slip is contained in a narrow band close to its optimal value. Two defined peaks are observed, each associated with a specific

friction coefficient. Moreover, limited distribution of longitudinal slip outside the stable area of the force-slip curve is identified.

Using the above-mentioned KPIs, Table 6 summarizes the obtained results. The minimum longitudinal acceleration at the transition reveals considerably less under-braking in response to the friction change for the NMPC controller compared to the threshold-based controller. Similarly, the time needed to regain steady state is also noticeably less. As a result, the mean deceleration value is sizably higher. Peak-to-peak metrics show how the first control cycle after the transition, is deeper for the benchmark. Lastly, although lateral stability is retained in both cases, the maximum yaw rate underlines the superiority of the NMPC design over the threshold-based one.

The summary of KPIs is shown in Fig. 13a. Front and rear peak-to-peak indicators were 78% and 50% lower respectively. Less torque variations also ensure a much shorter transition time (38% shorter). Lastly, an effect to keep under control regardless of the longitudinal transition performance is the maximum yaw rate. In this case the NMPC ensures 50% more yawing stability than the benchmark.

Fig. 13b shows the relative results for the dry asphalt braking from 130km/h to 0km/h. In this scenario, the NMPC main advantage is in the absence of first cycle overshoot, as particularly evident from the peak-to-peak indicators (approx. 50% better compared to the benchmark). Nevertheless, as a much larger portion of the braking manoeuvre is spent in stationary conditions, fewer percentage points of difference in steady-state performance also correspond to a remarkable improvement. The brake distance is reduced by more than 30% by the NMPC.

Jerk and pitch related indicators reveal an effect related to human factors (20% and 8% of the improvement correspondingly compared to the benchmark logic). The IACA demonstrates reduction of actuator wear (approx. 9% of the improvement).

Fig. 13c shows the relative results for the packed snow braking from 40km/h to 0km/h. Steady state performance indicators related to the proposed control were about 25% higher than the benchmark. The NMPC utilized more friction compared to the rule-based controller, increasing ABS efficiency. Jerk and pitch rate metrics are improved by approx. 65% and reduction of actuator wear (IACA) is improved by 29%.

V. CONCLUSION

Based on the presented state of the art in ABS control designs, it was decided to further investigate NMPC as a case study and compare it to the industry-used threshold-based control. To evaluate the proposed controller, a methodology similar to the industry-used assessment chain was applied: (i) a restricted set of manoeuvres were evaluated covering all possible ABS control fall-backs; (ii) a comprehensive set of key performance indicators (KPIs) was developed; (iii) a high-fidelity simulation setup (multibody vehicle model, rigid ring tire model, brake model, brake-pad interaction, etc.) was deployed to accurately replicates the braking behaviour from the field tests both at the vehicle level and actuator dynamics. The analysis showed that the proposed logic generally outperforms the threshold-based control on each of the simulated manoeuvres. The improvements are mainly due to a much smoother and precise control action. The NMPC destabilizes the wheel dynamics much less than the benchmark logic with its repeated control cycles (increase, decrease, and hold pressure). Additionally, there was a large improvement in the transient behaviour obtained with the NMPC controller. This was due to predictive nature of the controller. On average, the NMPC controller was able to improve by 75%, the first ABS control cycle, compared to the threshold-based controller. Similarly, following a transition in the friction coefficient, the NMPC was approximately 50% faster to recover from the friction transition. The NMPC controller improved the steady-state tracking by an average of 15%. Moreover, the NMPC controller also enhanced occupants' comfort up to 20% and reduced actuator wear by up to 30%. Regarding computational expenses, the proposed NMPC controller did not encounter any issues related to the solver failing to find a solution. Only minor real-time concerns at the beginning of the braking manoeuvre were observed as well as for the first few milliseconds after a friction transition occurred. Therefore, computational aspects are still open to future investigations. Lastly, the proposed NMPC requires a considerably lower number of tuning parameters (roughly two order of magnitude lower than the equivalent threshold-based logic).

REFERENCES

[1] K. Reif, *Brakes, Brake Control and Driver Assistance Systems: Function, Regulation and Components*. Weisbaden, Germany: Springer-Vieweg, 2014.

[2] G. Mauer, "A fuzzy logic controller for an ABS braking system," *IEEE Trans. Fuzzy Syst.*, vol. 3, no. 4, pp. 381–388, Nov. 1995.

[3] L. Austin and D. Morrey, "Recent advances in antilock braking systems and traction control systems," *Proc. Inst. Mech. Eng., D, J. Automobile Eng.*, vol. 214, no. 6, pp. 625–638, Jun. 2000.

[4] J. Wilkinson, C. W. Mousseau, and T. Klingler, "Brake response time measurement for a HIL vehicle dynamics simulator," SAE Tech. Paper 0148-7191, Apr. 2010.

[5] D. Wu, H. Ding, K. Guo, and Z. Wang, "Experimental research on the pressure following control of electro-hydraulic braking system," SAE Tech. Paper 0148-7191, Apr. 2014.

[6] S. Choi, J. Lee, and I. Hwang, "New generation ABS using linear flow control and motor speed control," *SAE Trans.*, pp. 237–242, 2003.

[7] J. Yao and W. Deng, "Active disturbance rejection adaptive control of hydraulic servo systems," *IEEE Trans. Ind. Electron.*, vol. 64, no. 10, pp. 8023–8032, Oct. 2017.

[8] Z. Yao, J. Yao, and W. Sun, "Adaptive RISE control of hydraulic systems with multilayer neural-networks," *IEEE Trans. Ind. Electron.*, vol. 66, no. 11, pp. 8638–8647, Nov. 2019.

[9] Y. Gao and M. Ehsani, "Electronic braking system of EV And HEV–integration of regenerative braking, automatic braking force control and ABS," *SAE Trans.*, pp. 576–582, Oct. 2010.

[10] J. Ko, S. Ko, H. Son, B. Yoo, J. Cheon, and H. Kim, "Development of brake system and regenerative braking cooperative control algorithm for automatic-transmission-based hybrid electric vehicles," *IEEE Trans. Veh. Technol.*, vol. 64, no. 2, pp. 431–440, Feb. 2015.

[11] J. Zhang, C. Lv, J. Gou, and D. Kong, "Cooperative control of regenerative braking and hydraulic braking of an electrified passenger car," *Proc. Inst. Mech. Eng., D, J. Automobile Eng.*, vol. 226, no. 10, pp. 1289–1302, Oct. 2012.
[12] N. Mutoh, "Driving and braking torque distribution methods for front- and rear-wheel-independent drive-type electric vehicles on roads with low friction coefficient," *IEEE Trans. Ind. Electron.*, vol. 59, no. 10, pp. 3919–3933, Oct. 2012.
[13] C. Lv, J. Zhang, Y. Li, and Y. Yuan, "Novel control algorithm of braking energy regeneration system for an electric vehicle during safety–critical driving maneuvers," *Energy Convers. Manage.*, vol. 106, pp. 520–529, Dec. 2015.
[14] Z. Zhang, R. Ma, L. Wang, and J. Zhang, "Novel PMSM control for anti-lock braking considering transmission properties of the electric vehicle," *IEEE Trans. Veh. Technol.*, vol. 67, no. 11, pp. 10378–10386, Nov. 2018.
[15] D. Savitski, V. Ivanov, K. Augsburg, T. Emmei, H. Fuse, H. Fujimoto, and L. Fridman, "Wheel slip control for the electric vehicle with in-wheel motors: Variable structure and sliding mode methods," *IEEE Trans. Ind. Electron.*, to be published.
[16] R. De Castro, R. E. Araújo, M. Tanelli, S. M. Savaresi, and D. Freitas, "Torque blending and wheel slip control in EVs with in-wheel motors," *Vehicle Syst. Dyn.*, vol. 50, no. 1, pp. 71–94, Jan. 2012.
[17] M. Gerard, W. Pasillas-Lépine, E. De Vries, and M. Verhaegen, "Adaptation of hybrid five-phase ABS algorithms for experimental validation," *IFAC Proc. Volumes*, vol. 43, no. 7, pp. 13–18, Jul. 2010.
[18] S. M. Savaresi, M. Tanelli, C. Cantoni, D. Charalambakis, F. Previdi, and S. Bittanti, "Slip-deceleration control in anti-lock braking systems," *IFAC Proc. Volumes*, vol. 38, no. 1, pp. 103–108, 2005.
[19] W. Pasillas-Lépine, "Hybrid modeling and limit cycle analysis for a class of five-phase anti-lock brake algorithms," *Vehicle Syst. Dyn.*, vol. 44, no. 2, pp. 173–188, Feb. 2006.
[20] S. M. Savaresi and M. Tanelli, *Active Braking Control Systems Design for Vehicles*. London, U.K.: Springer-Verlag, 2010.
[21] B. J. Ganzel, "Slip control boost braking system," U.S. Patents 2008 0 284 242 A1 Nov. 20, 2008.
[22] K. Berntorp, "Joint wheel-slip and vehicle-motion estimation based on inertial, GPS, and wheel-speed sensors," *IEEE Trans. Control Syst. Technol.*, vol. 24, no. 3, pp. 1020–1027, May 2016.
[23] W.-Y. Wang, I.-H. Li, M.-C. Chen, S.-F. Su, and S.-B. Hsu, "Dynamic slip-ratio estimation and control of antilock braking systems using an observer-based direct adaptive fuzzy-neural controller," *IEEE Trans. Ind. Electron.*, vol. 56, no. 5, pp. 1746–1756, May 2009.
[24] D. Nesic, A. Mohammadi, and C. Manzie, "A framework for extremum seeking control of systems with parameter uncertainties," *IEEE Trans. Autom. Control.*, vol. 58, no. 2, pp. 435–448, Feb. 2013.
[25] C. Lee, K. Hedrick, and K. Yi, "Real-time slip-based estimation of maximum tire-road friction coefficient," *IEEE/ASME Trans. Mechatronics*, vol. 9, no. 2, pp. 454–458, Jun. 2004.
[26] Z. Qi, S. Taheri, B. Wang, and H. Yu, "Estimation of the tyre–road maximum friction coefficient and slip slope based on a novel tyre model," *Vehicle Syst. Dyn.*, vol. 53, no. 4, pp. 506–525, Apr. 2015.
[27] V. Ivanov, B. Shyrokau, D. Savitski, J. Orus, R. Meneses, J.-M. Rodríguez-Fortún, J. Theunissen, and K. Janssen, "Design and testing of ABS for electric vehicles with individually controlled on-board motor drives," *SAE Int. J. Passenger Cars-Mech. Syst.*, vol. 7, no. 2, pp. 902–913, Aug. 2014.
[28] A. T. Van Zanten, R. Erhardt, K. Landesfeind, and G. Pfaff, "VDC systems development and perspective," *SAE Trans.*, pp. 424–444, 1998.
[29] U. Kiencke and L. Nielsen, *Automotive Control Systems: For Engine, Driveline, and Vehicle*, 2nd ed. Berlin, Germany: Springer-Verlag, 2005.
[30] S. Kerst, B. Shyrokau, and E. Holweg, "Reconstruction of wheel forces using an intelligent bearing," *SAE Int. J. Passenger Cars-Electron. Elect. Syst.*, vol. 9, no. 1, pp. 196–203, Apr. 2016.
[31] S. Kerst, B. Shyrokau, and E. Holweg, "A model-based approach for the estimation of bearing forces and moments using outer ring deformation," *IEEE Trans. Ind. Electron.*, vol. 67, no. 1, pp. 461–470, Jan. 2020.
[32] K. B. Singh, M. Ali Arat, and S. Taheri, "An intelligent tire based tire-road friction estimation technique and adaptive wheel slip controller for antilock brake system," *J. Dyn. Syst., Meas., Control*, vol. 135, no. 3, 2013, Art. no. 031002.
[33] M. Corno, M. Gerard, M. Verhaegen, and E. Holweg, "Hybrid ABS control using force measurement," *IEEE Trans. Control Syst. Technol.*, vol. 20, no. 5, pp. 1223–1235, Sep. 2012.
[34] S. Kerst, B. Shyrokau, and E. Holweg, "Anti-lock braking control based on bearing load sensing," in *Proc. EuroBrake*, Dresden, Germany, 2015, pp. 4–6.
[35] A. A. Aly, E.-S. Zeidan, A. Hamed, and F. Salem, "An antilock-braking systems (ABS) control: A technical review," *Intell. Control Automat.*, vol. 2, no. 3, p. 186, 2011.
[36] V. Ivanov, D. Savitski, and B. Shyrokau, "A survey of traction control and antilock braking systems of full electric vehicles with individually controlled electric motors," *IEEE Trans. Veh. Technol.*, vol. 64, no. 9, pp. 3878–3896, Sep. 2015.
[37] R. B. GmbH., K. Reif, and K.-H. Dietsche, *Automotive Handbook*. Gerlingen, Germany: Robert Bosch, 2014.
[38] M. Vignati and E. Sabbioni, "Force-based braking control algorithm for vehicles with electric motors," *Vehicle Syst. Dyn.*, pp. 1–19, Jun. 2019.
[39] A. G. Ulsoy, H. Peng, and M. Çakmakci, *Automotive Control Systems*. Cambridge, U.K.: Cambridge Univ. Press, 2012.
[40] T. Johansen, J. Kalkkuhl, J. Ludemann, and I. Petersen, "Hybrid control strategies in ABS," in *Proc. Amer. Control Conf.*, vol. 2, 2001, pp. 1704–1705.
[41] I. Ait-Hammouda and W. Pasillas-Lépine, "On a class of eleven-phase anti-lock brake algorithms robust with respect to discontinuous transitions of road characteristics," *IFAC Proc. Volumes*, vol. 37, no. 21, pp. 551–556, Dec. 2004.
[42] J. Layne, K. Passino, and S. Yurkovich, "Fuzzy learning control for antiskid braking systems," *IEEE Trans. Control Syst. Technol.*, vol. 1, no. 2, pp. 122–129, Jun. 1993.
[43] J. Cabrera, A. Ortiz, J. Castillo, and A. Simon, "A fuzzy logic control for antilock braking system integrated in the IMMa tire test bench," *IEEE Trans. Veh. Technol.*, vol. 54, no. 6, pp. 1937–1949, Nov. 2005.
[44] W. Lennon and K. Passino, "Intelligent control for brake systems," *IEEE Trans. Control Syst. Technol.*, vol. 7, no. 2, pp. 188–202, Mar. 1999.
[45] V. G. Ivanov, V. B. Algin, and B. N. Shyrokau, "Intelligent control for ABS application with identification of road and environmental properties," *Int. J. Vehicle Auton. Syst.*, vol. 4, no. 1, p. 44, 2006.
[46] S.-W. Kim and J.-J. Lee, "Design of a fuzzy controller with fuzzy sliding surface," *Fuzzy Sets Syst.*, vol. 71, no. 3, pp. 359–367, May 1995.
[47] C.-M. Lin and C.-F. Hsu, "Self-learning fuzzy sliding-mode control for antilock braking systems," *IEEE Trans. Control Syst. Technol.*, vol. 11, no. 2, pp. 273–278, Mar. 2003.
[48] B.-J. Choi, S.-W. Kwak, and B. K. Kim, "Design of a single-input fuzzy logic controller and its properties," *Fuzzy Sets Syst.*, vol. 106, no. 3, pp. 299–308, Sep. 1999.
[49] Y. Lee and S. Zak, "Designing a genetic neural fuzzy antilock-brake-system controller," *IEEE Trans. Evol. Comput.*, vol. 6, no. 2, pp. 198–211, Apr. 2002.
[50] S. Baglio, L. Fortuna, S. Graziani, and G. Muscato, "Membership function shape and the dynamic behaviour of fuzzy systems," *Int. J. Adapt. Control Signal Process.*, vol. 8, no. 4, pp. 369–377, Jul. 1994.
[51] B. N. Shyrokau and V. G. Ivanov, "Alterable fuzzy sets in automotive control applications," *Int. J. Model., Identificat. Control*, vol. 3, no. 3, pp. 305–307, 2008.
[52] G. Kokes and T. Singh, "Adaptive fuzzy logic control of an anti-lock braking system," in *Proc. IEEE Int. Conf. Control Appl.*, vol. 1, Jan. 2003, pp. 646–651.
[53] L. Davis, G. Puskorius, F. Yuan, and L. Feldkamp, "Neural network modeling and control of an anti-lock brake system," in *Proc. Intell. Vehicles Symp.*, Jan. 2003, pp. 179–184.
[54] C.-M. Lin and C.-F. Hsu, "Neural-network hybrid control for antilock braking systems," *IEEE Trans. Neural Netw.*, vol. 14, no. 2, pp. 351–359, Mar. 2003.
[55] A. Poursamad, "Adaptive feedback linearization control of antilock braking systems using neural networks," *Mechatronics*, vol. 19, no. 5, pp. 767–773, Aug. 2009.
[56] J. O. Pedro, O. A. Dahunsi, and O. T. Nyandoro, "Direct adaptive neural control of antilock braking systems incorporated with passive suspension dynamics," *J. Mech. Sci. Technol.*, vol. 26, no. 12, pp. 4115–4130, Dec. 2012.
[57] Y. Li, K. H. Ang, and G. C. Y. Chomg, "PID control system analysis and design: Problems, remedies, and future directions," *IEEE Control Syst. Mag.*, vol. 26, no. 1, pp. 32–41, Feb. 2006.
[58] D. Savitski, D. Schleinin, V. Ivanov, and K. Augsburg, "Robust continuous wheel slip control with reference adaptation: Application to the brake system with decoupled architecture," *IEEE Trans. Ind. Informat.*, vol. 14, no. 9, pp. 4212–4223, Sep. 2018.

[59] T. Johansen, I. Petersen, J. Kalkkuhl, and J. Ludemann, "Gain-scheduled wheel slip control in automotive brake systems," *IEEE Trans. Control Syst. Technol.*, vol. 11, no. 6, pp. 799–811, Nov. 2003.

[60] T. A. Johansen, I. Petersen, and O. Slupphaug, "Explicit sub-optimal linear quadratic regulation with state and input constraints," *Automatica*, vol. 38, no. 7, pp. 1099–1111, Jul. 2002.

[61] I. Petersen, "Wheel slip control in ABS brakes using gain scheduled optimal control with constraints," Ph.D. dissertation, Norwegian Univ. Sci. Technol., Trondheim, Norway, 2003.

[62] M.-C. Wu and M.-C. Shih, "Simulated and experimental study of hydraulic anti-lock braking system using sliding-mode PWM control," *Mechatronics*, vol. 13, no. 4, pp. 331–351, May 2003.

[63] S. Drakunov, U. Ozguner, P. Dix, and B. Ashrafi, "ABS control using optimum search via sliding modes," *IEEE Trans. Control Syst. Technol.*, vol. 3, no. 1, pp. 79–85, Mar. 1995.

[64] A. Will, S. Hui, and S. Zak, "Sliding mode wheel slip controller for an antilock braking system," *Int. J. Vehicle Des.*, vol. 19, no. 4, pp. 523–539, 1998.

[65] H. Sira-Ramírez, "On the sliding mode control of nonlinear systems," *Syst. Control Lett.*, vol. 19, no. 4, pp. 303–312, 1992.

[66] P. Wellstead and N. Pettit, "Analysis and redesign of an antilock brake system controller," *IEE Proc.-Control Theory Appl.*, vol. 144, no. 5, pp. 413–426, Sep. 1997.

[67] K. R. Buckholtz, "Reference input wheel slip tracking using sliding mode control," *SAE Trans.*, pp. 477–483, 2002.

[68] C. Unsal and P. Kachroo, "Sliding mode measurement feedback control for antilock braking systems," *IEEE Trans. Control Syst. Technol.*, vol. 7, no. 2, pp. 271–281, Mar. 1999.

[69] K. Buckholtz, "Approach angle-based switching function for sliding mode control design," in *Proc. Amer. Control Conf.*, vol. 3, May 2002, pp. 2368–2373.

[70] A. Harifi, A. Aghagolzadeh, G. Alizadeh, and M. Sadeghi, "Designing a sliding mode controller for slip control of antilock brake systems," *Transp. Res. C, Emerg. Technol.*, vol. 16, no. 6, pp. 731–741, Dec. 2008.

[71] R. De Castro, R. E. Araujo, and D. Freitas, "Wheel slip control of EVs based on sliding mode technique with conditional integrators," *IEEE Trans. Ind. Electron.*, vol. 60, no. 8, pp. 3256–3271, Aug. 2013.

[72] T. Shim, S. Chang, and S. Lee, "Investigation of sliding-surface design on the performance of sliding mode controller in antilock braking systems," *IEEE Trans. Veh. Technol.*, vol. 57, no. 2, pp. 747–759, Mar. 2008.

[73] X. Han, E. Fridman, and S. Spurgeon, "Sliding-mode control of uncertain systems in the presence of unmatched disturbances with applications," *Int. J. Control*, vol. 83, no. 12, pp. 2413–2426, Dec. 2010.

[74] M. Tanelli and A. Ferrara, "Enhancing robustness and performance via switched second order sliding mode control," *IEEE Trans. Autom. Control.*, vol. 58, no. 4, pp. 962–974, Apr. 2013.

[75] E. Kayacan, Y. Oniz, and O. Kaynak, "A grey system modeling approach for sliding-mode control of antilock braking system," *IEEE Trans. Ind. Electron.*, vol. 56, no. 8, pp. 3244–3252, Aug. 2009.

[76] Y. Jing, Y.-E. Mao, G. M. Dimirovski, Y. Zheng, and S. Zhang, "Adaptive global sliding mode control strategy for the vehicle antilock braking systems," in *Proc. Amer. Control Conf.*, Jun. 2009, pp. 769–773.

[77] T. Kawabe, M. Nakazawa, I. Notsu, and Y. Watanabe, "A sliding mode controller for wheel slip ratio control system," *Vehicle Syst. Dyn.*, vol. 27, nos. 5–6, pp. 393–408, Jun. 1997.

[78] C. Poussot-Vassal, "Discussion on: 'Combining slip and deceleration control for brake-by-wire control systems: A sliding-mode approach,'" *Eur. J. Control*, vol. 13, no. 6, pp. 612–615, Jan. 2007.

[79] M. Tanelli, R. Sartori, and S. M. Savaresi, "Sliding mode slip-deceleration control for brake-by-wire control systems," *IFAC Proc. Volumes*, vol. 40, no. 10, pp. 135–142, 2007.

[80] K. Glover and J. C. Doyle, "A state space approach to H_∞ optimal control," in *Three Decades of Mathematical System Theory*. Berlin, Germany: Springer, 1989, pp. 179–218.

[81] Y. B. Yan, H. Wu, and W. Q. Wang, "Research on robust control of anti-locked braking system of vehicles," *Appl. Mech. Mater.*, vols. 543–547, pp. 1504–1509, Mar. 2014.

[82] S. Ç. Başlamışli, İ. E. Köse, and G. Anlas, "Robust control of anti-lock brake system," *Vehicle Syst. Dyn.*, vol. 45, no. 3, pp. 217–232, Mar. 2007.

[83] Y.-E. Mao, Y. Zheng, Y. Jing, G. M. Dimirovski, and S. Hang, "An LMI approach to slip ratio control of vehicle Antilock braking systems," in *Proc. Amer. Control Conf.*, Jun. 2009, pp. 3350–3354.

[84] A. Bemporad and M. Morari, "Robust model predictive control: A survey," in *Robustness in Identification and Control*. London, U.K.: Springer, 1999, pp. 207–226.

[85] A. Richards and J. How, "Robust stable model predictive control with constraint tightening," in *Proc. Amer. Control Conf.*, 2006, pp. 1–6.

[86] D. Q. Mayne, E. C. Kerrigan, E. J. Van Wyk, and P. Falugi, "Tube-based robust nonlinear model predictive control," *Int. J. Robust Nonlinear Control*, vol. 21, no. 11, pp. 1341–1353, Jul. 2011.

[87] F. Oldewurtel, C. N. Jones, and M. Morari, "A tractable approximation of chance constrained stochastic MPC based on affine disturbance feedback," in *Proc. 47th IEEE Conf. Decis. Control*, Dec. 2008, pp. 4731–4736.

[88] A. Wächter and L. T. Biegler, "On the implementation of an interior-point filter line-search algorithm for large-scale nonlinear programming," *Math. Program.*, vol. 106, no. 1, pp. 25–57, Mar. 2006.

[89] H. J. Ferreau, C. Kirches, A. Potschka, H. G. Bock, and M. Diehl, "QpOASES: A parametric active-set algorithm for quadratic programming," *Math. Program. Comput.*, vol. 6, no. 4, pp. 327–363, Dec. 2014.

[90] S. Anwar, "Yaw stability control of an automotive vehicle via generalized predictive algorithm," in *Proc. Amer. Control Conf.*, Aug. 2005, pp. 435–440.

[91] S. Anwar and B. Ashrafi, "A predictive control algorithm for an anti-lock braking system," *SAE Trans.*, pp. 484–490, 2002.

[92] M. Hasankhansari, M. Yaghoobi, and A. Abaspour, "Independent model generalized predictive controller design for antilock braking system," *Int. J. Comput. Appl.*, vol. 114, no. 1, pp. 18–23, Mar. 2015.

[93] G. Valencia-Palomo and J. Rossiter, "Programmable logic controller implementation of an auto-tuned predictive control based on minimal plant information," *ISA Trans.*, vol. 50, no. 1, pp. 92–100, Jan. 2011.

[94] H. Mirzaeinejad and M. Mirzaei, "A novel method for non-linear control of wheel slip in anti-lock braking systems," *Control Eng. Pract.*, vol. 18, no. 8, pp. 918–926, Aug. 2010.

[95] D. K. Yoo and L. Wang, "Model based wheel slip control via constrained optimal algorithm," in *Proc. IEEE 22nd Int. Symp. Intell. Control*, Oct. 2007, pp. 1239–1246.

[96] M. S. Basrah, E. Siampis, E. Velenis, D. Cao, and S. Longo, "Wheel slip control with torque blending using linear and nonlinear model predictive control," *Vehicle Syst. Dyn.*, vol. 55, no. 11, pp. 1665–1685, Nov. 2017.

[97] A. Zanelli, A. Domahidi, J. Jerez, and M. Morari, "FORCES NLP: An efficient implementation of interior-point methods for multistage nonlinear nonconvex programs," *Int. J. Control*, vol. 93, no. 1, pp. 13–29, Jan. 2020.

[98] D. Tavernini, F. Vacca, M. Metzler, D. Savitski, V. Ivanov, P. Gruber, A. E. H. Karci, M. Dhaens, and A. Sorniotti, "An explicit nonlinear model predictive ABS controller for electro-hydraulic braking systems," *IEEE Trans. Ind. Electron.*, to be published.

[99] C. Mi, H. Lin, and Y. Zhang, "Iterative learning control of antilock braking of electric and hybrid vehicles," *IEEE Trans. Veh. Technol.*, vol. 54, no. 2, pp. 486–494, Mar. 2005.

[100] J.-S. Lin and W.-E. Ting, "Nonlinear control design of anti-lock braking systems with assistance of active suspension," *IET Control Theory Appl.*, vol. 1, no. 1, pp. 343–348, Jan. 2007.

[101] M. Tanelli, A. Astolfi, and S. M. Savaresi, "Robust nonlinear output feedback control for brake by wire control systems," *Automatica*, vol. 44, no. 4, pp. 1078–1087, Apr. 2008.

[102] E. De Vries, A. Fehn, and D. Rixen, "Flatness-based model inverse for feed-forward braking control," *Vehicle Syst. Dyn.*, vol. 48, no. 1, pp. 353–372, Dec. 2010.

[103] M.-B. Radac and R.-E. Precup, "Data-driven model-free slip control of anti-lock braking systems using reinforcement Q-learning," *Neurocomputing*, vol. 275, pp. 317–329, Jan. 2018.

[104] C. F. Verdier, R. Babuška, B. Shyrokau, and M. Mazo, Jr., "Near optimal control with reachability and safety guarantees," *IFAC-PapersOnLine*, vol. 52, no. 11, pp. 230–235, 2019.

[105] D. Cao, X. Song, and M. Ahmadian, "Editors' perspectives: Road vehicle suspension design, dynamics, and control," *Vehicle Syst. Dyn.*, vol. 49, nos. 1–2, pp. 3–28, Feb. 2011.

[106] B. Shyrokau, D. Wang, D. Savitski, K. Hoepping, and V. Ivanov, "Vehicle motion control with subsystem prioritization," *Mechatronics*, vol. 30, pp. 297–315, Sep. 2015.

[107] D. Ariens, B. Houska, H. Ferreau, and F. Logist. (2011). *ACADO for MATLAB User's Manual*. Accessed: Dec. 20, 2019. [Online]. Available: http://acado.sourceforge.net/doc/pdf/acado_matlab_manual.pdf

[108] B. Houska, H. J. Ferreau, and M. Diehl, "An auto-generated real-time iteration algorithm for nonlinear MPC in the microsecond range," *Automatica*, vol. 47, no. 10, pp. 2279–2285, Oct. 2011.
[109] G. Ostermeyer, "On the dynamics of the friction coefficient," *Wear*, vol. 254, no. 9, pp. 852–858, May 2003.
[110] B. Shyrokau, D. Wang, K. Augsburg, and V. Ivanov, "Vehicle dynamics with brake hysteresis," *Proc. Inst. Mech. Eng., D, J. Automobile Eng.*, vol. 227, no. 2, pp. 139–150, 2013.
[111] A. Belhocine and W. Z. W. Omar, "Three-dimensional finite element modeling and analysis of the mechanical behavior of dry contact slipping between the disc and the brake pads," *Int. J. Adv. Manuf. Technol.*, vol. 88, nos. 1–4, pp. 1035–1051, Jan. 2017.
[112] A. Belhocine, "FE prediction of thermal performance and stresses in an automotive disc brake system," *Int. J. Adv. Manuf. Technol.*, vol. 89, nos. 9–12, pp. 3563–3578, Apr. 2017.
[113] A. Belhocine and W. Z. W. Omar, "CFD analysis of the brake disc and the wheel house through air flow: Predictions of Surface heat transfer coefficients (STHC) during braking operation," *J. Mech. Sci. Technol.*, vol. 32, no. 1, pp. 481–490, Jan. 2018.
[114] F. Pretagostini, B. Shyrokau, and G. Berardo, "Anti-lock braking control design using a nonlinear model predictive approach and wheel information," in *Proc. IEEE Int. Conf. Mechatronics (ICM)*, vol. 1, Mar. 2019, pp. 525–530.

FRANCESCO PRETAGOSTINI received the B.Sc. degree in mechatronics from the University of Rome Tor Vergata, Italy, in 2016, and the M.Sc. degree *(cum laude)* in vehicle engineering from the Delft University of Technology, The Netherlands, in 2018, with a focus on vehicle dynamics and controls. He performed his thesis project in Toyota Motor Europe, Belgium, on topics related to brake system design and advanced brake controllers. Since September 2018, he has been a Performance Engineer with Ferrari, Italy, focusing on innovation topics related to advanced vehicle control, new sensor, and actuator development.

LAURA FERRANTI received the M.Sc. degree *(cum laude)* in control engineering from the University of Rome Tor Vergata, Italy, in 2012, and the Ph.D. degree in control engineering from the Delft University of Technology, The Netherlands, in 2017. She is currently an Assistant Professor with the Cognitive Robotics Department, Delft University of Technology. She has coauthored the best paper in multirobot systems at the 2019 International Conference on Robotics and Automation (ICRA). Her research interests include optimization and optimal control, model predictive control, embedded optimization-based control with application in flight control, maritime transportation, robotics, and automotive.

GIOVANNI BERARDO received the M.Sc. degree *(cum laude)* in mechanical engineering from the University of Rome Tor Vergata, Italy, in 1998. In 2003, he joined Toyota Motor Europe taking various operational and management responsibilities in Europe and Japan, where he is in charge of chassis systems of mass production vehicles. Since 2017, he has been managed the European Team developing controls for the vehicle motion of conventional and automated driving vehicles. His research interests include resistance of structures employed in oil and gas transportation, he moved to an engineering role in the automotive industry.

VALENTIN IVANOV received the Mech.Eng., Ph.D., and D.Sc. degrees in automotive engineering from the Belarusian National Technical University, Minsk, Belarus, in 1992, 1997, and 2006, respectively, and the Dr.Ing. habil. degree in automotive engineering from the Technische Universität Ilmenau (TUIL), Ilmenau, Germany, in 2017. From 1998 to 2007, he was an Assistant Professor, an Associate Professor, and a Full Professor with the Department of Automotive Engineering, Belarusian National Technical University. He is currently the European Project Coordinator with the Automotive Engineering Group, TUIL. His research interests include vehicle dynamics, electric vehicles, automotive control systems, and chassis design.

BARYS SHYROKAU received the Dipl.Eng. degree *(cum laude)* in mechanical engineering from Belarusian National Technical University, Belarus, in 2004, and the joint Ph.D. degree in control engineering from Nanyang Technological University, Singapore, in 2015, and Technical University Munich, Germany. He is currently an Assistant Professor with the Section of Intelligent Vehicles, Department of Cognitive Robotics, Delft University of Technology, The Netherlands. His research interests are vehicle dynamics and control, motion comfort, and driving simulator technology. He received the Scholarship and Award from FISITA, DAAD, SINGA, ISTVS, and CADLM.